Welcome to Palm Springs!

2018 SCEC Annual Meeting

- Assess progress towards SCEC5 goals
- Broadcast Science Plan (RFP) to recruit research
- Modify Science Plan as necessary

Poster Sessions: dedicated *prime* time to nucleate ideas and forge collaborations

New This Year! Lightning Talks at 3:00 Tomorrow

SCEC5 Planning Committee

PC Chairs
Greg Beroza, *Chair*
Judi Chester, *Vice-Chair*

Disciplinary Committees

Seismology
Yehuda Ben-Zion
Jamie Steidl

Tectonic Geodesy
Gareth Funning
Manoochehr Shirzaei

Earthquake Geology
Mike Oskin
Whitney Behr

Computational Science
Eric Dunham
Ricardo Taborda

Interdisciplinary Focus Groups

FARM
Nadia Lapusta
Nick Beeler

SDOT
Kaj Johnson
Bridget Smith-Konter

EFP
Max Werner
Ned Field

GM
Domniki Asimaki
Annemarie Baltay

EEII
Jack Baker
Jon Stewart

CXM
Liz Hearn
Scott Marshall

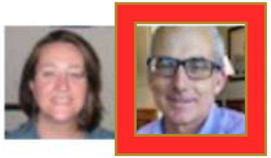

SAFS
Michele Cooke
Ramon Arrowsmith

Special Projects
Christine Goulet
Phil Maechling

SCEC5 Science Accomplishments

(Core + Special Projects)

Gregory C. Beroza
Co-Director

Christine A. Goulet
Executive Science Director
for Special Projects

Theme A. Modeling the Fault System

1. Stress and Deformation Over Time
2. Special Fault Study Areas: Focus on Earthquake Gates
3. Community Models
4. Data-Intensive Computing

www.scec.org/research/cxm

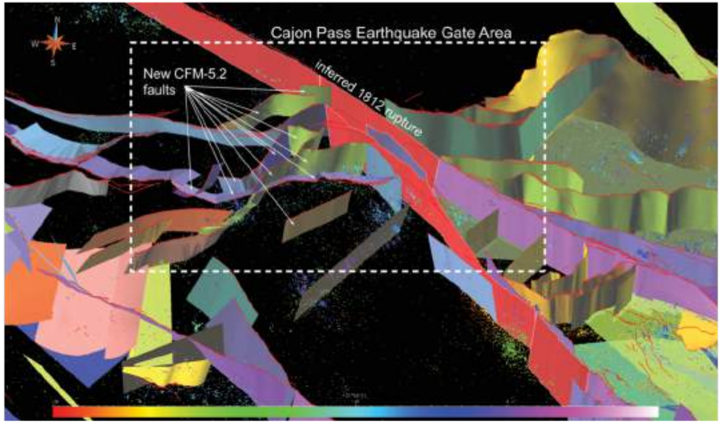

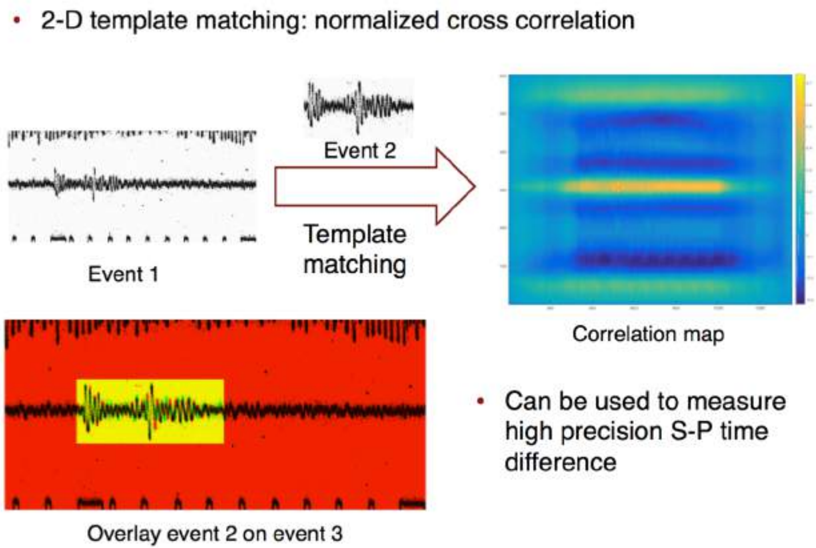

1. Stress and Deformation Over Time

How many surface clasts needed to constrain alluvial fan exposure age?

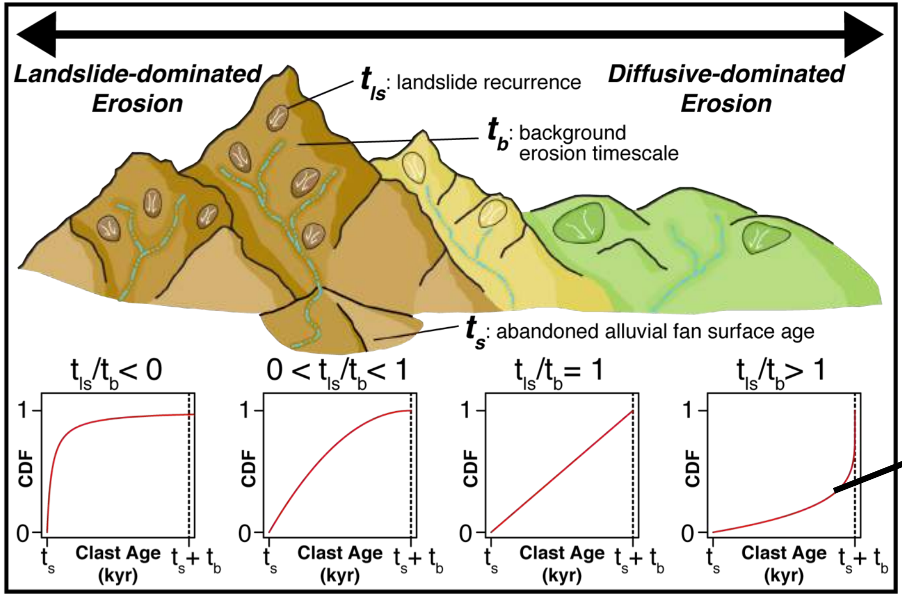

Synthetic tests show ~14 clasts needed. Few published sites meet this standard

Example Distribution

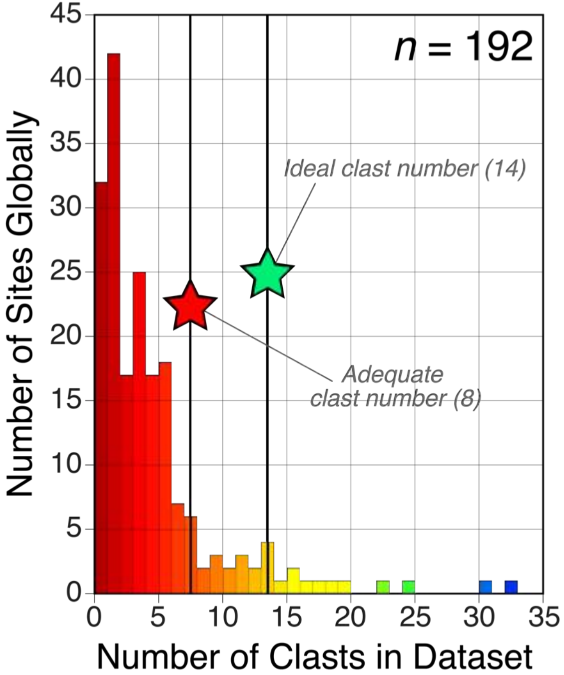

Landslide erosion-dominated catchments = concave-down distributions

Background erosion-dominated catchments = concave-up distributions

Prush and Oskin (Poster #231)

Recalculated dates of the two most recent surface ruptures on the southernmost San Andreas fault

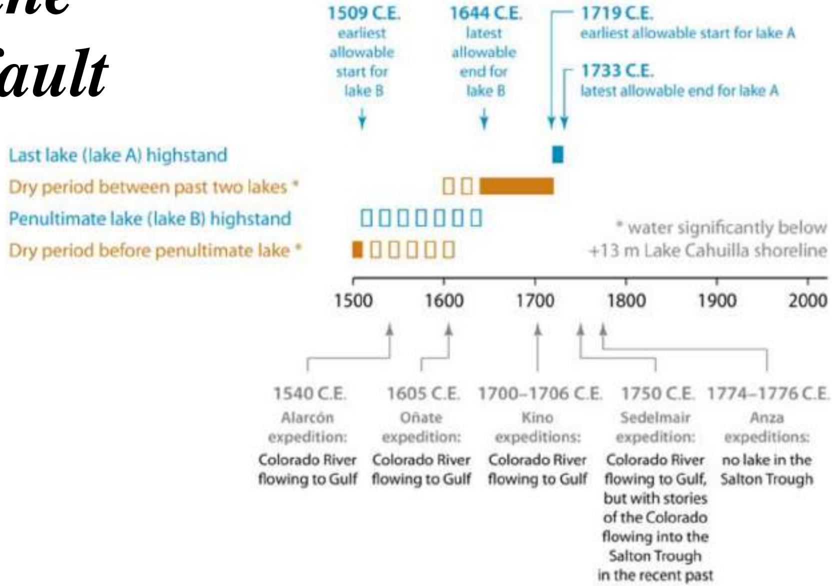

RESEARCH ARTICLE | JULY 17, 2018

Dates of the Two Most Recent Surface Ruptures on the Southernmost San Andreas Fault Recalculated by Precise Dating of Lake Cahuilla Dry Periods

Thomas K. Rockwell; Aron J. Meltzner; Erik C. Haaker

Bulletin of the Seismological Society of America (2018)
https://doi.org/10.1785/0120170392

Analysis constrains the open interval to 300 years with 150 yr recurrence for the two MRE that is consistent with 180 yr recurrence from record of earlier events

Slip rate summary: ~steady strain accumulation and release

Southern California Earthquake Center

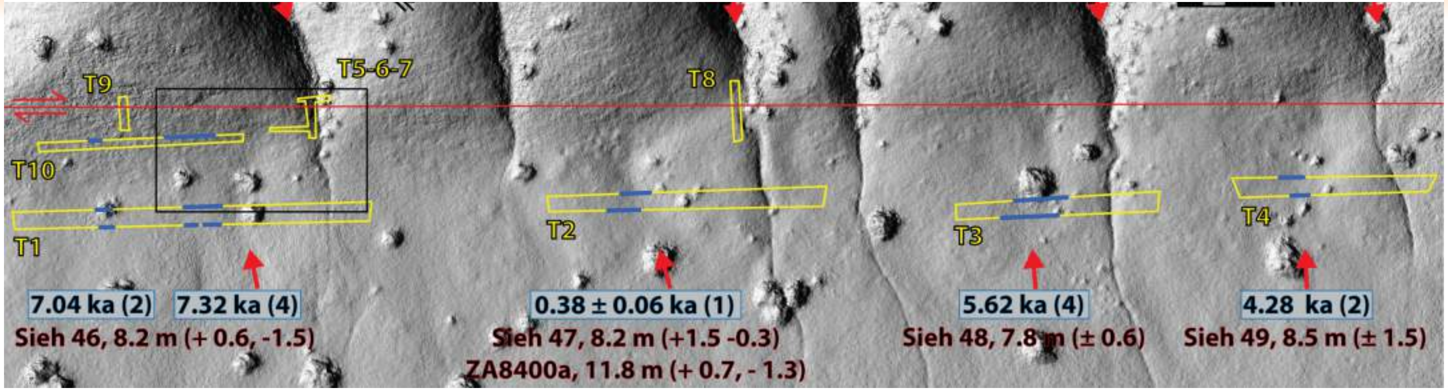

31.6 +5.9/-4.3 mm/yr

Multiple new offset rates along the San Andreas Fault in the Carrizo Plain consistent with earlier work and are fairly steady.

RESEARCH ARTICLE | JANUARY 30, 2018

The Age and Origin of Small Offsets at Van Matre Ranch along the San Andreas Fault in the Carrizo Plain, California

J. Barrett Salisbury; J Ramón Arrowsmith; Nathan Brown; Thomas Rockwell; Sinan Akciz; Lisa Grant Ludwig

Bulletin of the Seismological Society of America (2018) 108 (2): 639-653.

https://doi.org/10.1785/0120170162

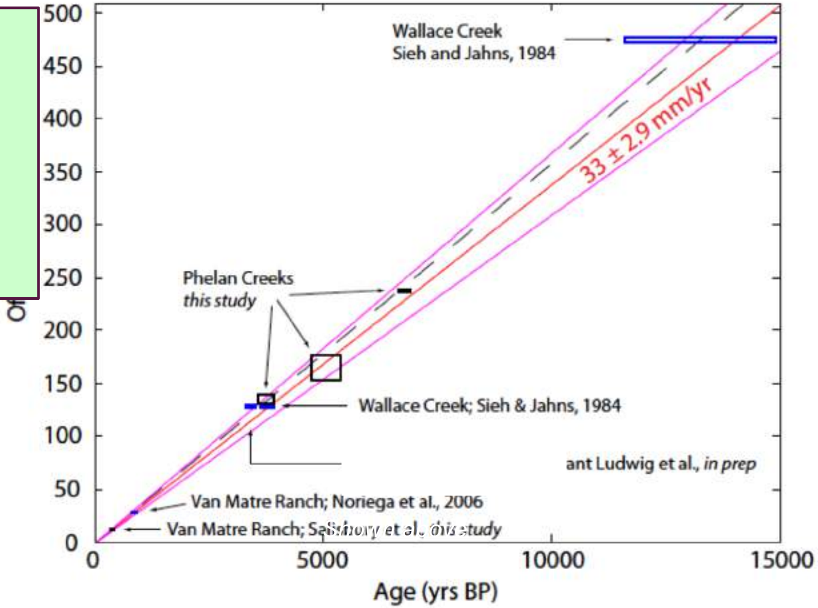

Slip History of the Sierra Madre fault

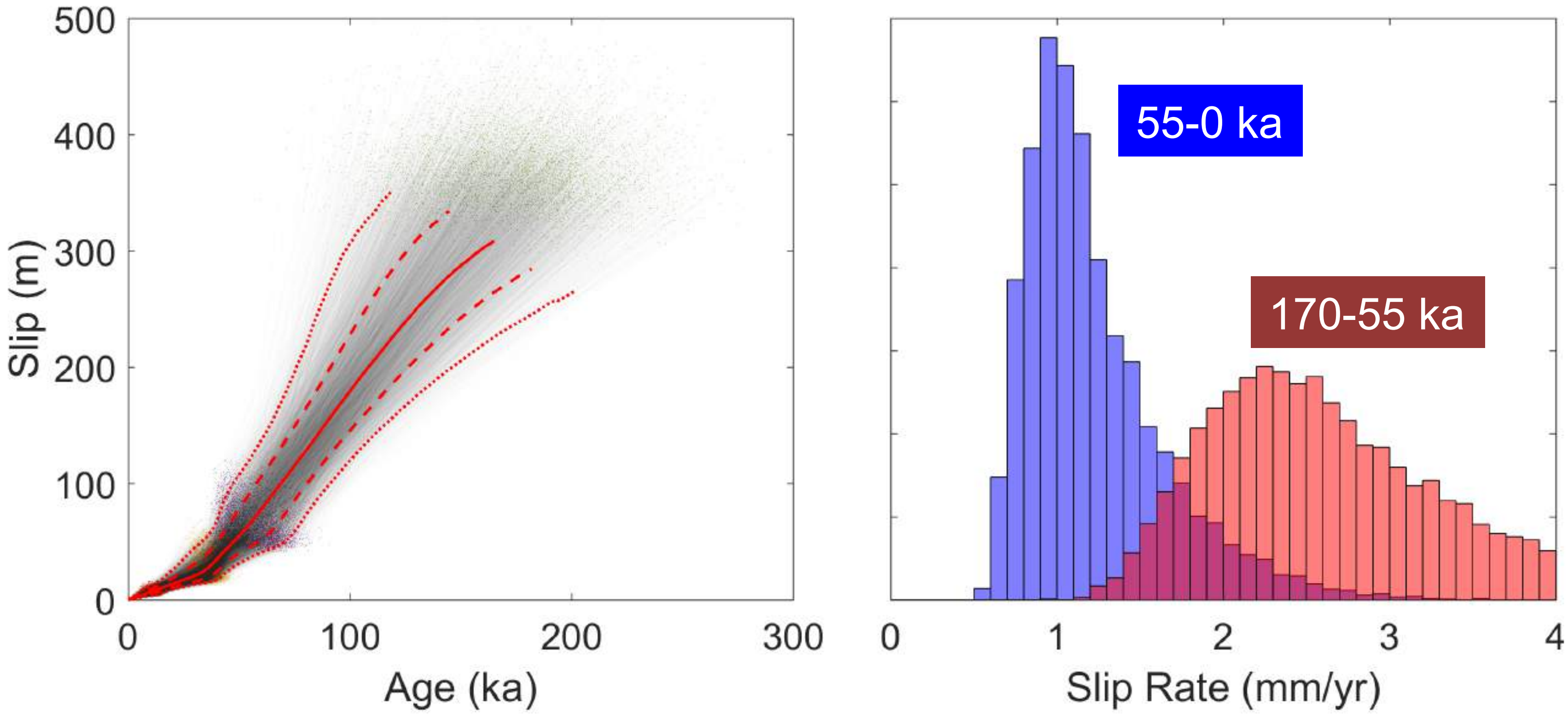

(Poster #254)
PIs: Burgette, Lifton & Scharer

Sierra Madre Fault shows a decrease in slip rate by factor of ~2 in last ~60 ka.

SSAF creep rate modulations

InSAR data spanning 1992–2017 show decreasing creep rate with time

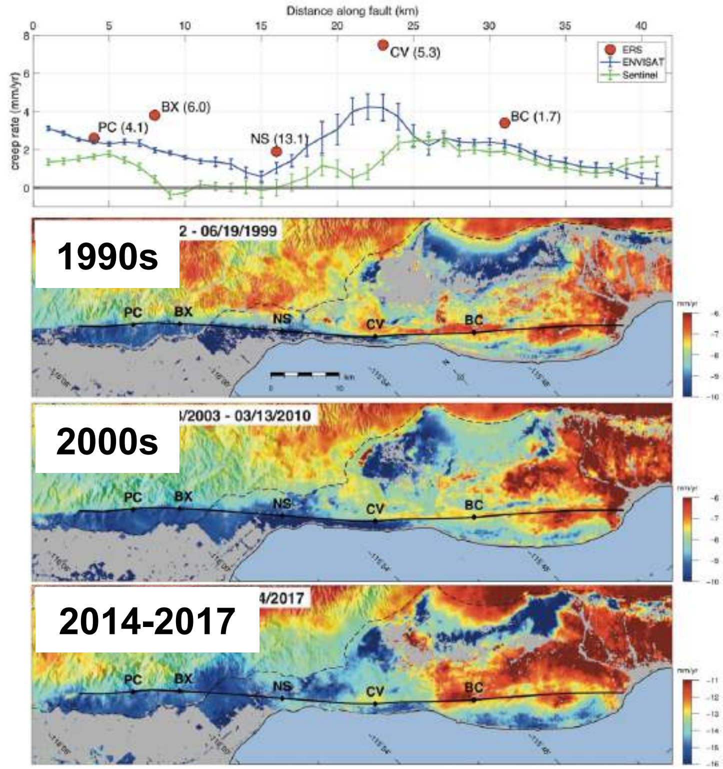

Positive correlation between Coulomb stress changes from M>7 events and SSAF decadal creep rates estimated from InSAR

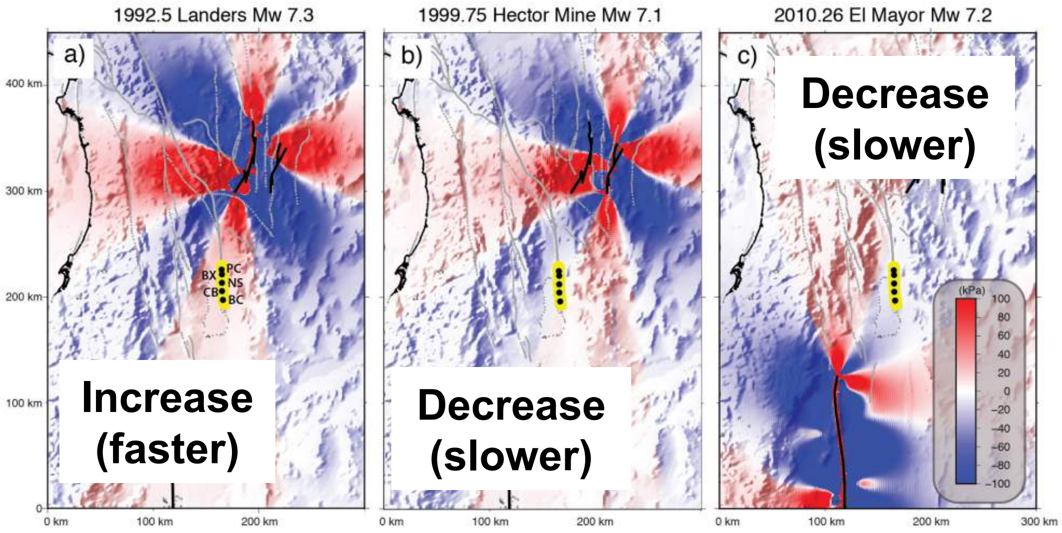

Xu et al., GRL, in press (2018)

SC/EC

Seasonal Stress Changes

Southern California Earthquake Center

Horizontal seasonal signals with dilatational strains

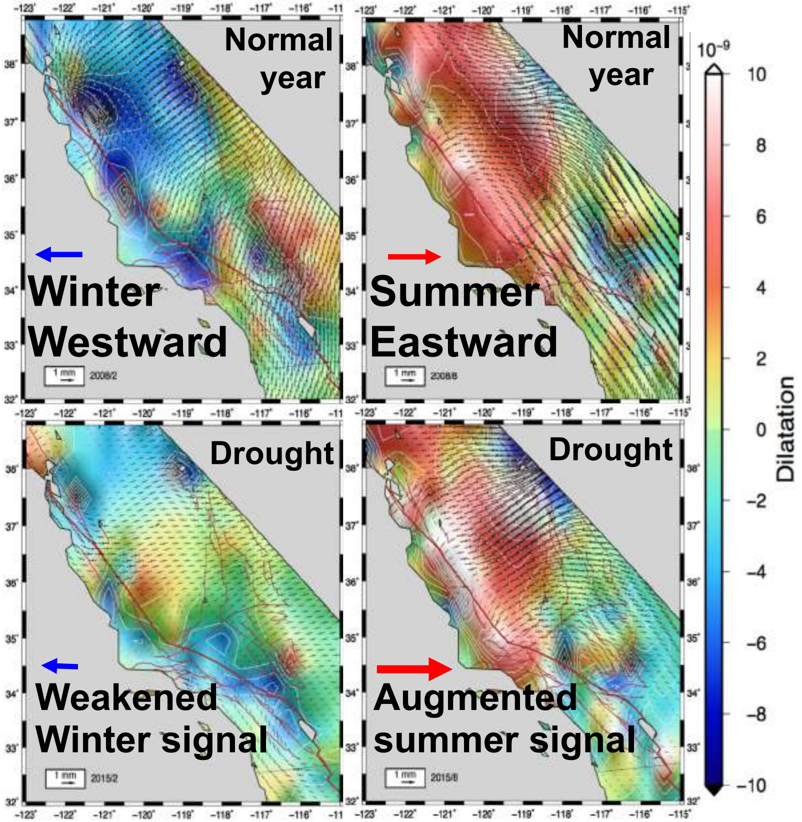

Associated Coulomb stress changes on the right lateral strike-slip faults

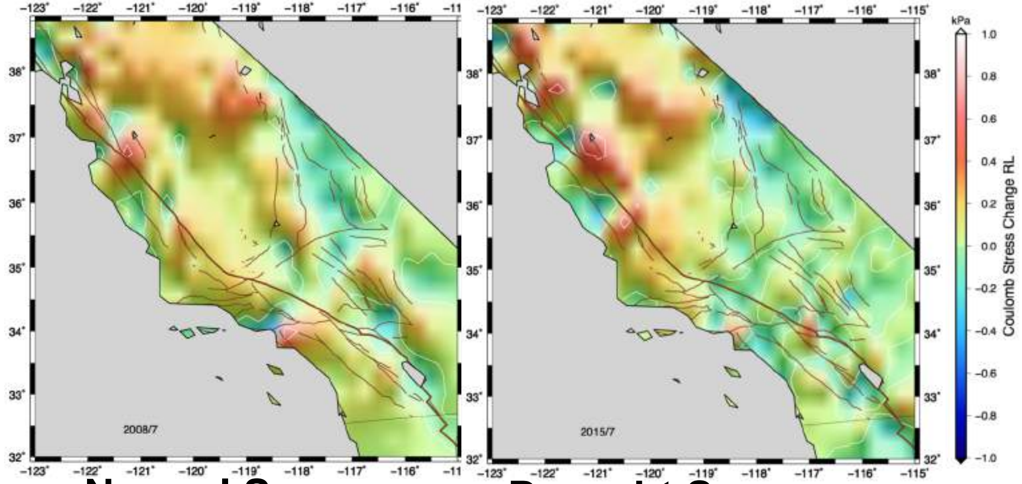

Normal Summer Stress patterns

Drought Summer Stress patterns

During the drought, the augmented summer signals escalate the summer stress patterns along the San Andreas Fault zone and the Eastern California Shear Zone.

Kim, Bahadori, and Holt. (Poster #156)

Nontectonic trigger of South Napa EQ?

Dilatational strain (left) and Coulomb stress (right) estimated from CGPS

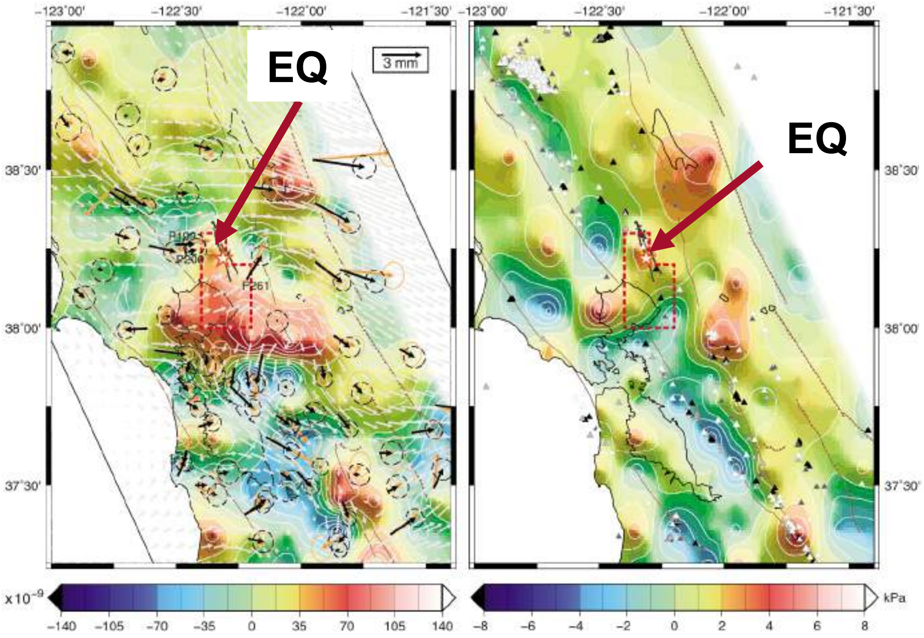

2014/08/24
***M* 6.1**

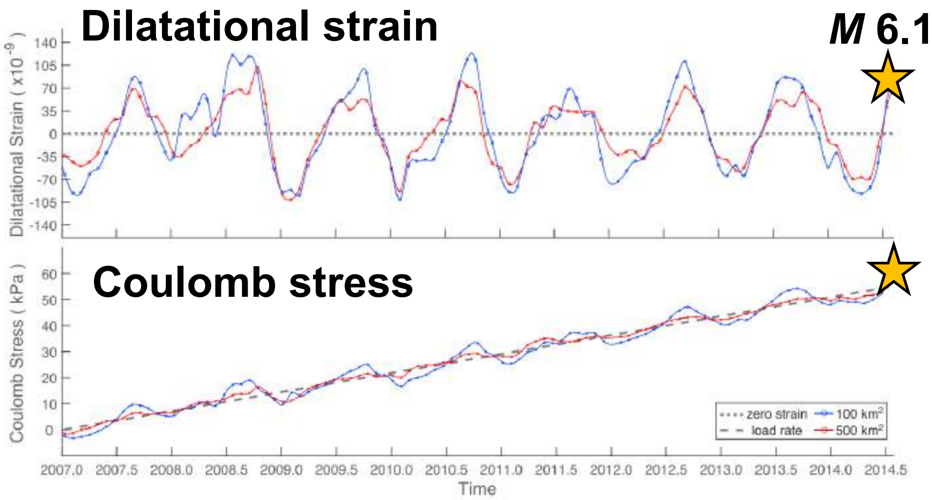

Majority of the dilatational strain is attributed to groundwater changes; its late summer peak is a plausible trigger for the August 24th event.

Kraner et al., JGR (2018)

Southern San Cayetano Fault Slip Rate

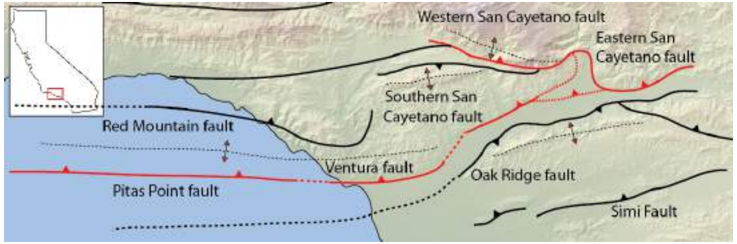

SSCF connects Ventura and San Cayetano fault at the surface

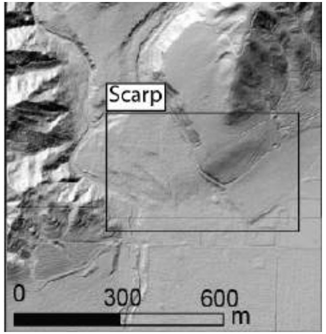

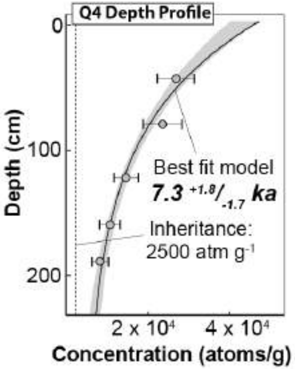

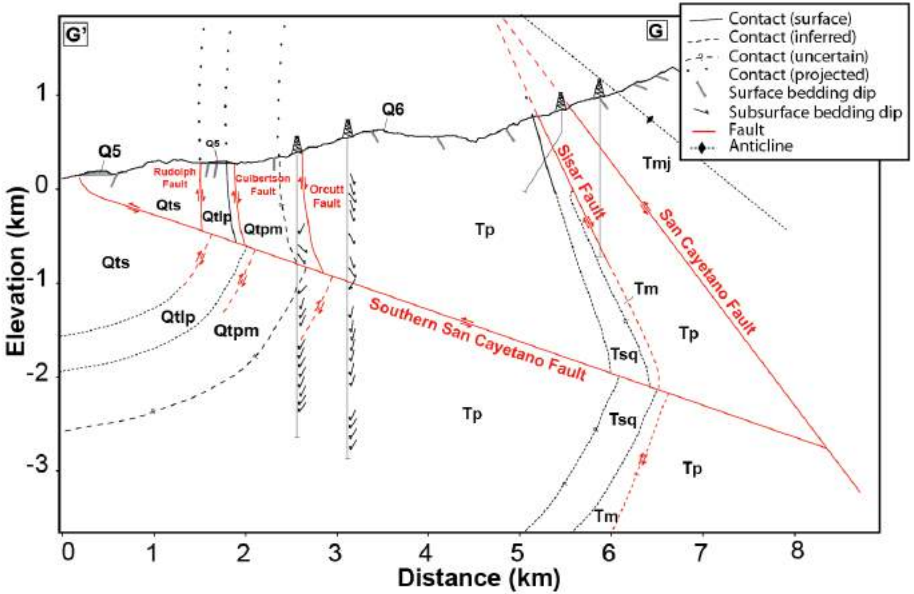

Subsurface data indicates SSCF is a low-angle (20°) thrust

Hughes et al. (Poster #253)

SSCF links Ventura and San Cayetano faults, likely ruptures in large multi-fault events. Holocene slip rate of 1.3 +0.5/-0.3 mm/yr.

2. Earthquake Gate

Stress Inversion of Focal Mechanisms

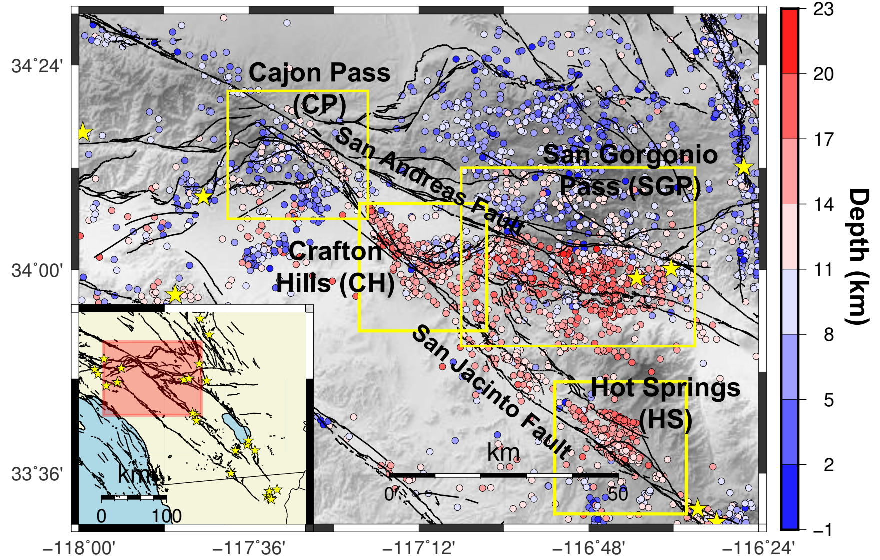

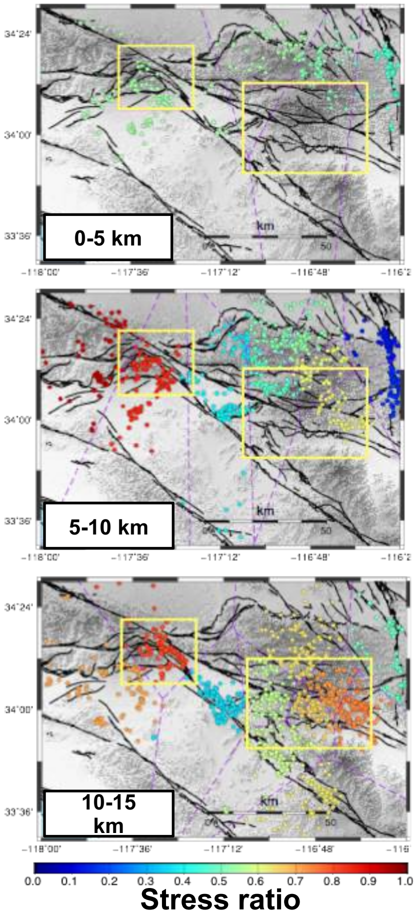

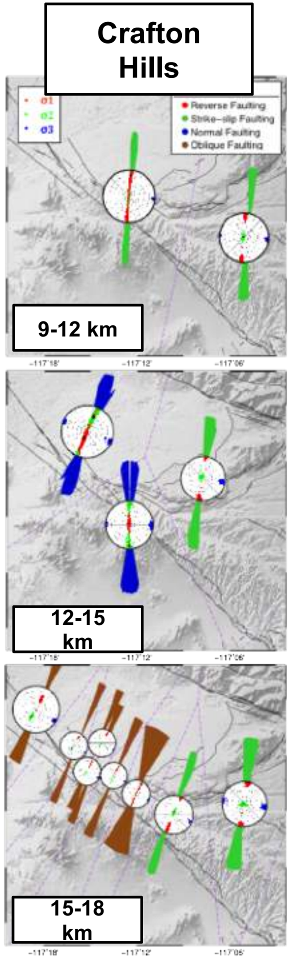

- Variations of stress ratio ($R = \frac{\sigma_1 - \sigma_2}{\sigma_1 - \sigma_3}$) in areas with high topography, similar feature is seen in CP, SGP and HS
- Significant rotation of maximum horizontal compressional stress (S_{Hmax}) with depth in Crafton Hills
- Numerical simulations aid in understanding the results

Abolfathian, Johnson, Ben-Zion *(Poster #155)*

Odd normal slip focal mechanisms in the San Bernardino basin could be due to deep creep on the northern San Jacinto fault

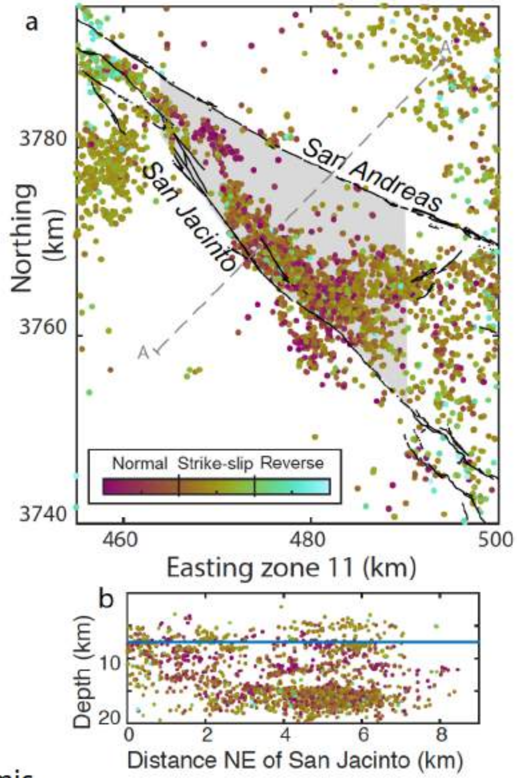

Deep Creep Model

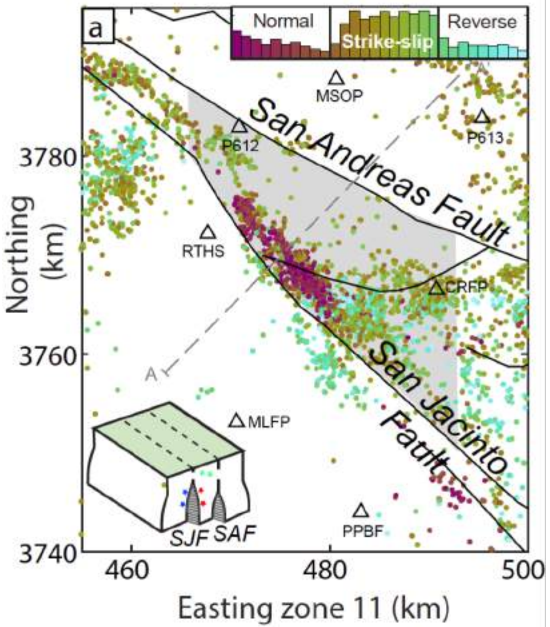

Geophysical Research Letters
AN AGU JOURNAL
Research Letter | Full Access

Off-fault Focal Mechanisms not Representative of Interseismic Fault Loading Suggest Deep Creep on the Northern San Jacinto Fault

M. L. Cooke, J. L. Beyer

First published: 30 August 2018 | https://doi.org/10.1029/2018GL078932

Focal mechanisms may not provide reliable indicators of interseismic loading off the faults have some degree of creep

Strain rate and earthquake cycle stress accumulation influenced by crustal rigidity variations: Cajon Pass

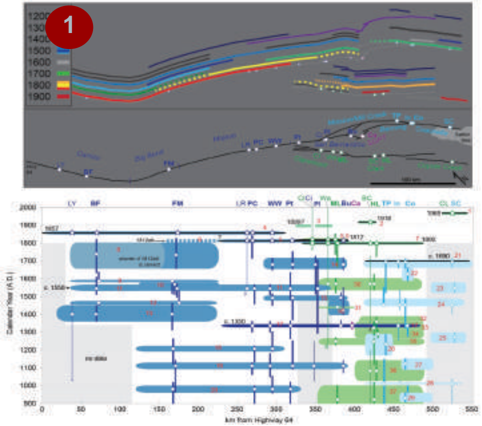

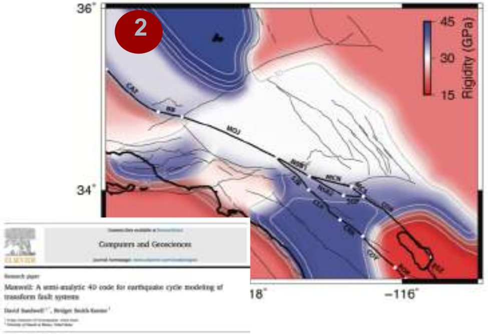

New paleoseisimic rupture estimates **(1)** + new 4D crustal deformation model that accounts for heterogeneous crustal rigidity **(2)**

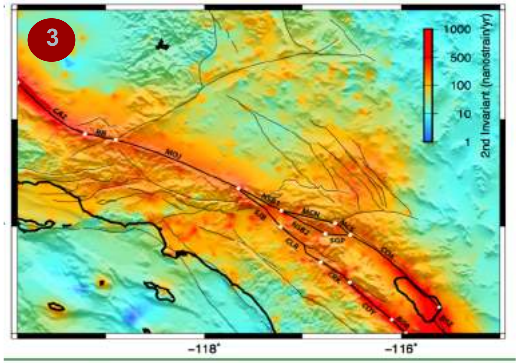

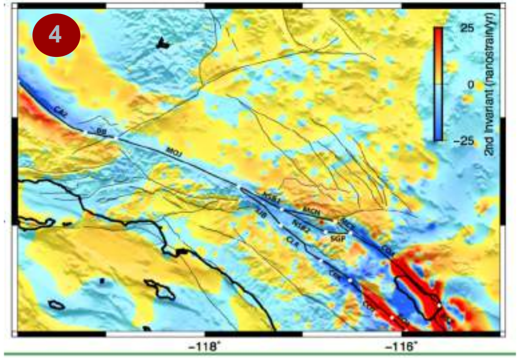

Updates to present-day strain rate model **(3)** and changes due to crustal rigidity variations **(4)**; A decrease in rigidity → increase in strain rate

Ward, Smith-Konter, Xu, and Sandwell; Poster #260

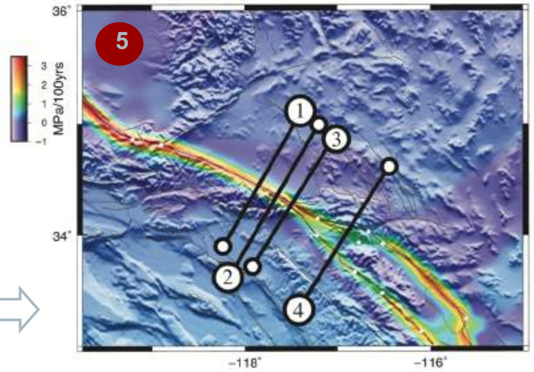

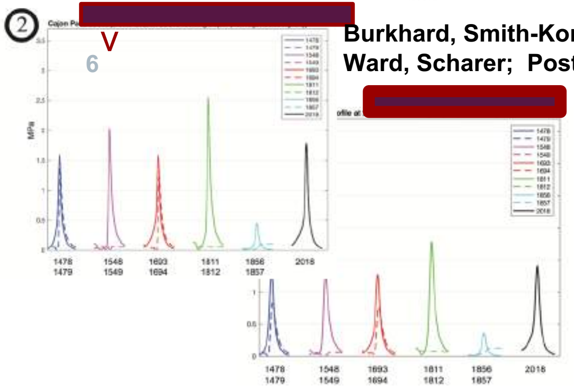

Burkhard, Smith-Konter, Ward, Scharer; Poster #262

Stress accumulation rates **(5)** and event thresholds **(6)** are reduced along the Cajon Pass when crustal rigidity variations are introduced.

3. Community Models

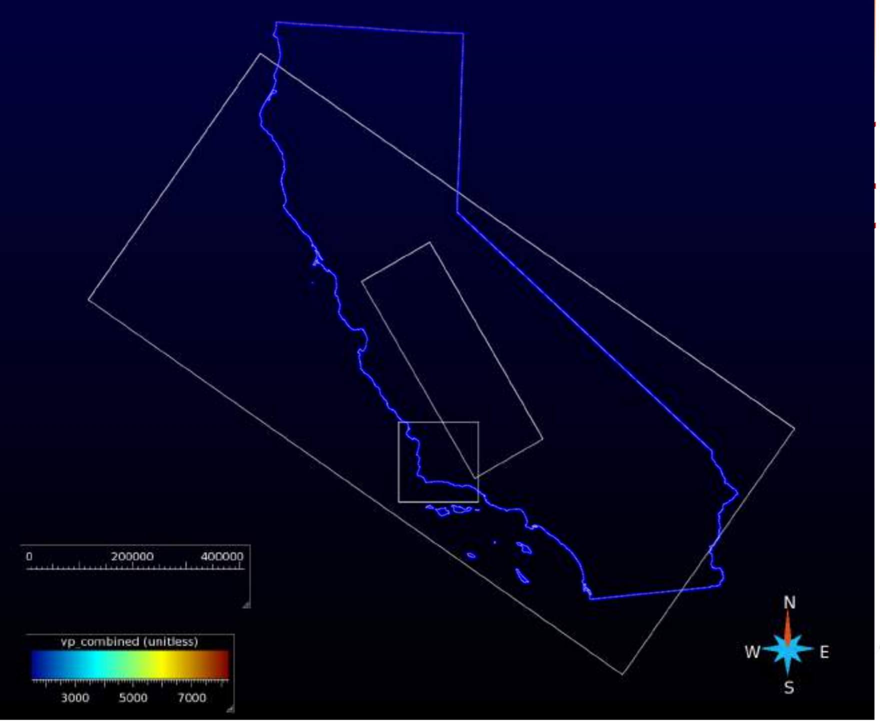

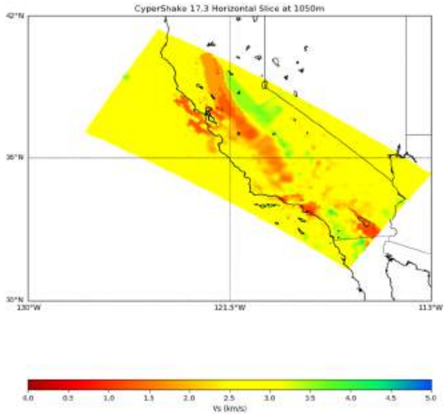

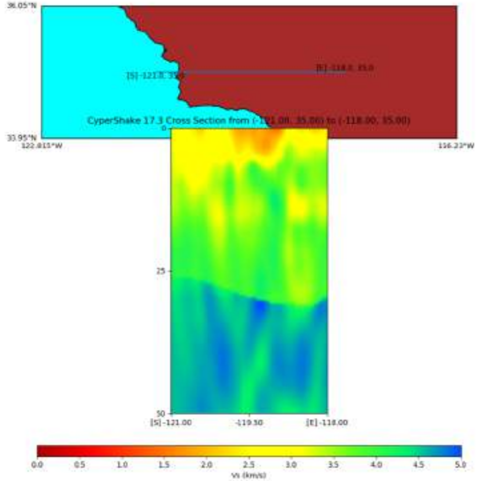

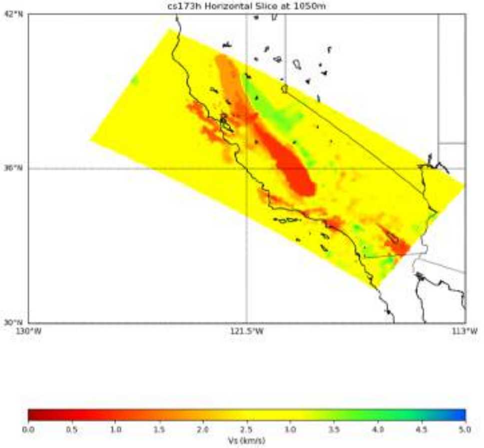

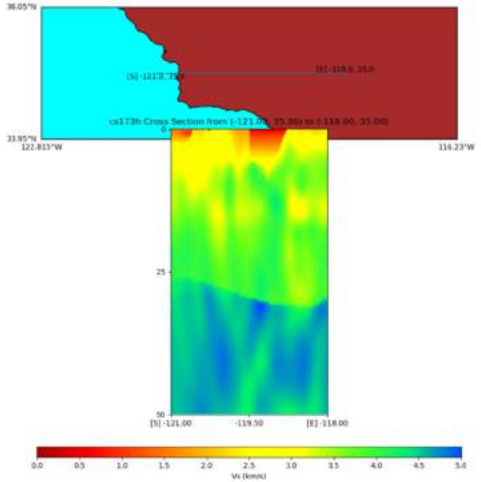

(Above) SCEC has developed a new Central California Velocity Model (coverage region indicated by larger white rectangle), called CS173-H, that includes detailed representations of the San Joaquin Basin (smaller white rectangle - center) and the Santa Maria Basin (small white square).

(Right) Vs at 1K depth and horizontal cross section of the CS173 velocity model show the original CS173 velocity model (Top Row) and the updated CS173-H velocity model (Bottom Row) which includes the San Joaquin and Santa Maria Basins.

SCEC

Southern California Earthquake Center

Updated SCEC CFM v.5.2 Fault Representations for 2018

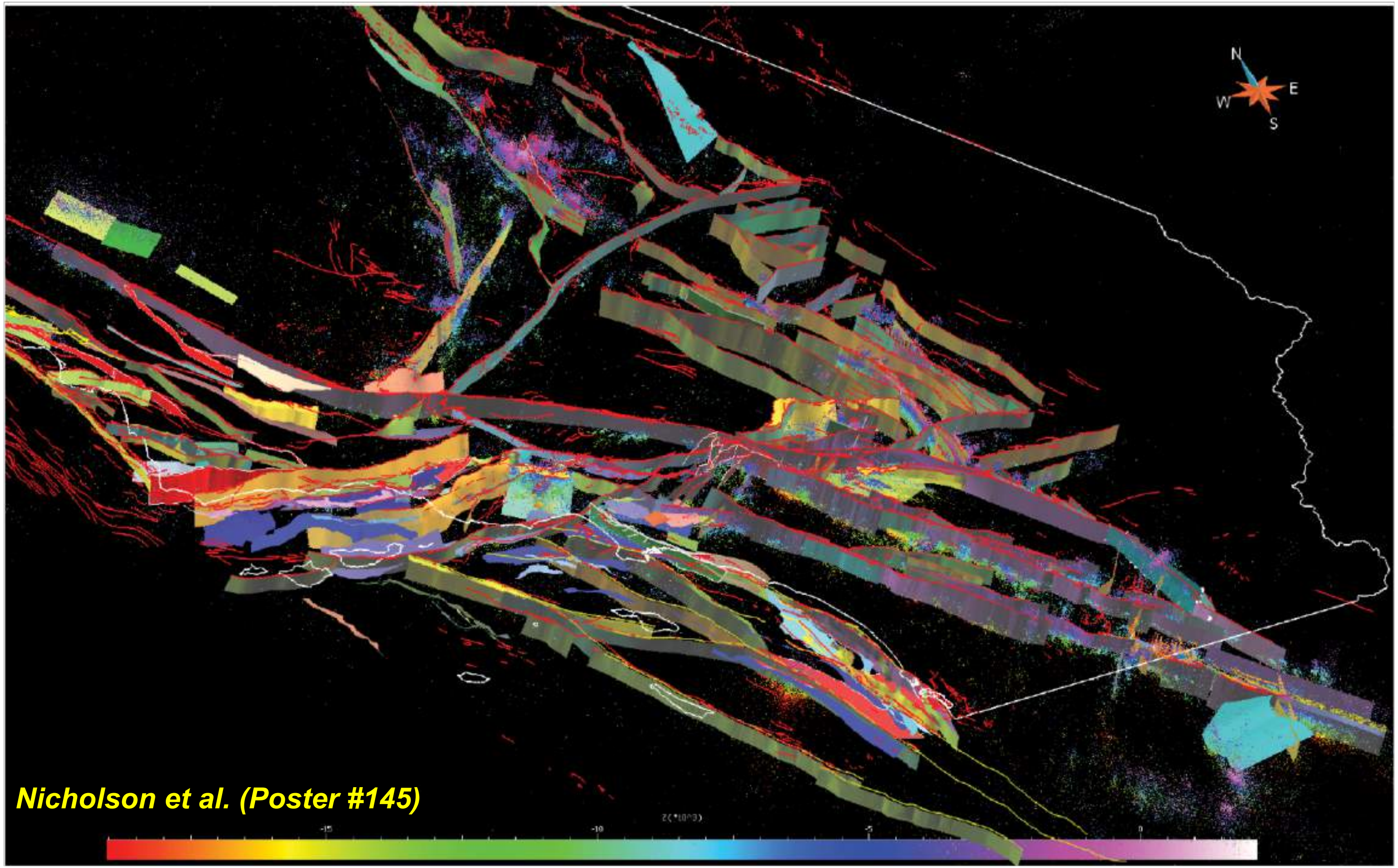

New CFM webpage @ ***https://www.scec.org/research/cfm***

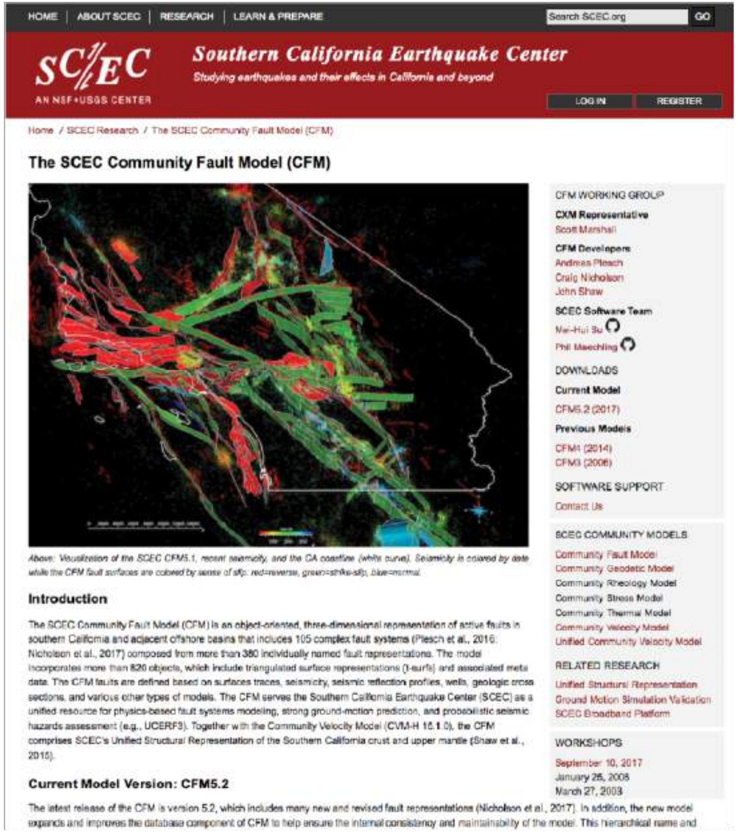

HOME | ABOUT SCEC | RESEARCH | LEARN & PREPARE — Search SCEC.org — GO

SC/EC — AN NSF+USGS CENTER

Southern California Earthquake Center

Studying earthquakes and their effects in California and beyond

LOG IN | REGISTER

Home / SCEC Research / The SCEC Community Fault Model (CFM)

The SCEC Community Fault Model (CFM)

Above: Visualization of the SCEC CFM5.1, recent seismicity, and the CA coastline (white curve). Seismicity is colored by date while the CFM fault surfaces are colored by sense of slip: red=reverse, green=strike-slip, blue=normal.

Introduction

The SCEC Community Fault Model (CFM) is an object-oriented, three-dimensional representation of active faults in southern California and adjacent offshore basins that includes 105 complex fault systems (Plesch et al., 2016; Nicholson et al., 2017) composed from more than 380 individually named fault representations. The model incorporates more than 820 objects, which include triangulated surface representations (t-surfs) and associated meta data. The CFM faults are defined based on surfaces traces, seismicity, seismic reflection profiles, wells, geologic cross sections, and various other types of models. The CFM serves the Southern California Earthquake Center (SCEC) as a unified resource for physics-based fault systems modeling, strong ground-motion prediction, and probabilistic seismic hazards assessment (e.g., UCERF3). Together with the Community Velocity Model (CVM-H 15.1.0), the CFM comprises SCEC's Unified Structural Representation of the Southern California crust and upper mantle (Shaw et al., 2015).

Current Model Version: CFM5.2

The latest release of the CFM is version 5.2, which includes many new and revised fault representations (Nicholson et al., 2017). In addition, the new model expands and improves the database component of CFM to help ensure the internal consistency and maintainability of the model. This hierarchical name and

CFM WORKING GROUP

CXM Representative
Scott Marshall

CFM Developers
Andreas Plesch
Craig Nicholson
John Shaw

SCEC Software Team
Mei-Hui Su
Phil Maechling

DOWNLOADS

Current Model
CFM5.2 (2017)

Previous Models
CFM4 (2014)
CFM3 (2006)

SOFTWARE SUPPORT
Contact Us

SCEC COMMUNITY MODELS
Community Fault Model
Community Geodetic Model
Community Rheology Model
Community Stress Model
Community Thermal Model
Community Velocity Model
Unified Community Velocity Model

RELATED RESEARCH
Unified Structural Representation
Ground Motion Simulation Validation
SCEC Broadband Platform

WORKSHOPS
September 10, 2017
January 26, 2008
March 27, 2003

CFM fault surfaces reformatted for viewing in 3D with free MoVE Viewer app are available to download

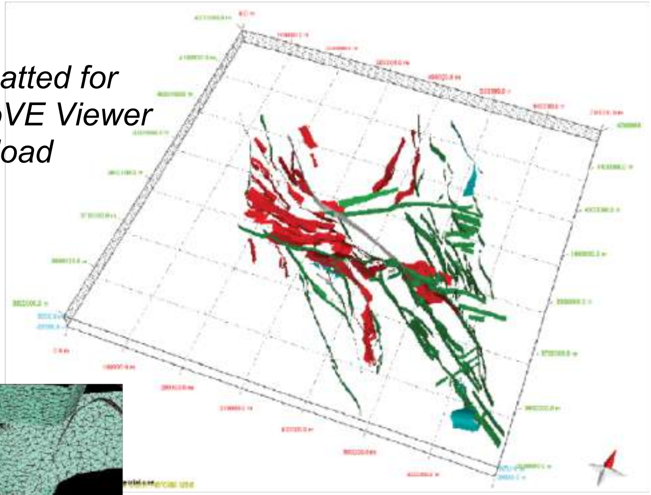

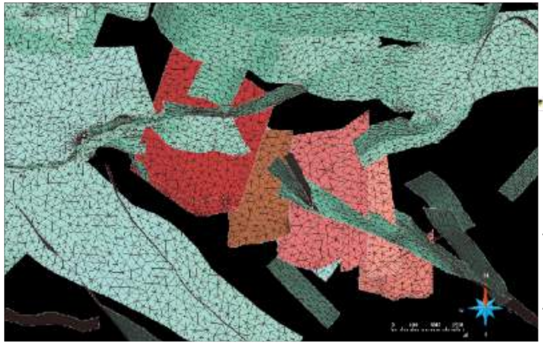

Example of regular-gridded re-meshed CFM fault surfaces at 1000-m intervals for the LA Basin area

Nicholson et al. (Poster #145)

Webpage provides user downloads of CFM 3D fault sets, regular-gridded re-meshed surfaces to facilitate modeling, GIS map representations in X3D, and tools for viewing and evaluating the updated CFM-v5.2 fault set in 3D.

Geologic Framework for the SCEC CRM

- Updated GF province definitions
- Registered province boundaries to SCEC USR features
- Generated shape and lat-lon files for province boundaries
- Generated preliminary 1D lithological profiles for all GF provinces

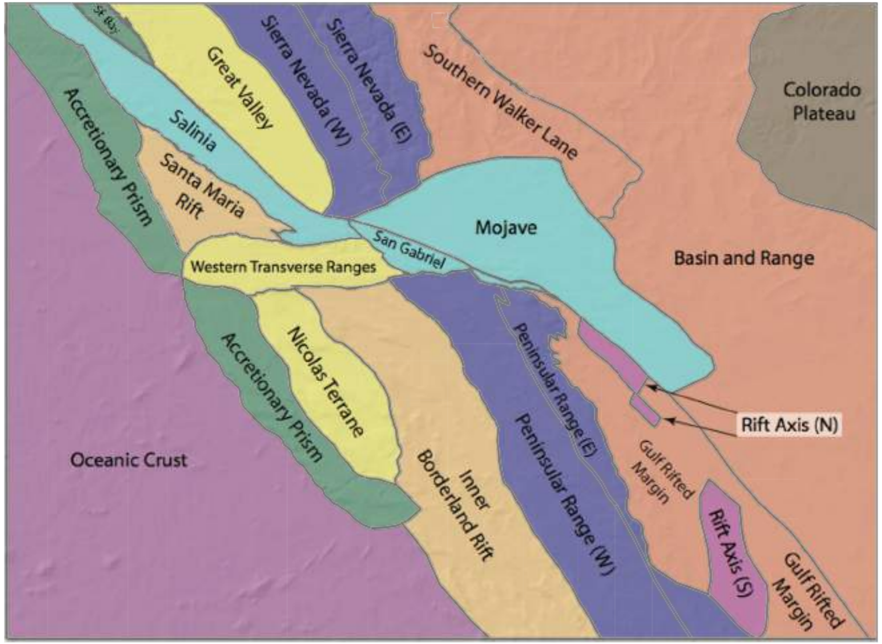

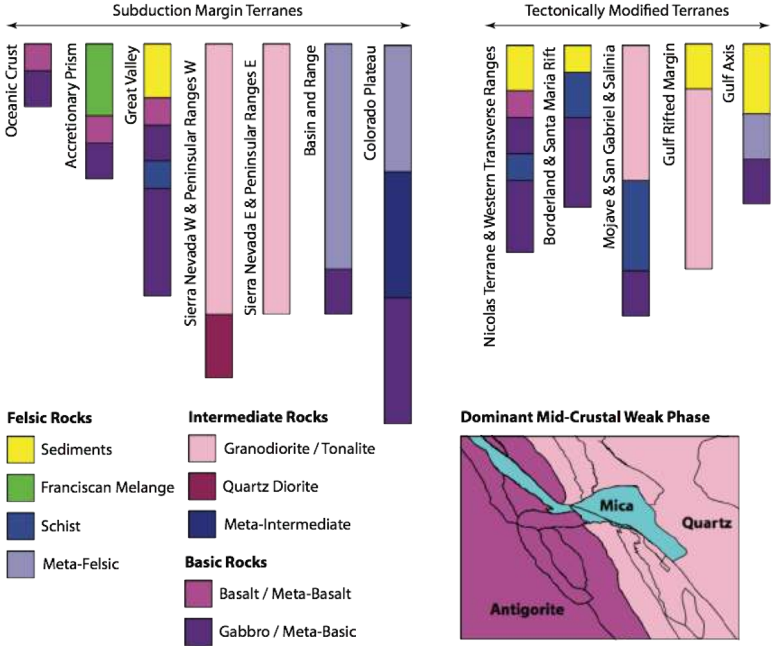

Legg and Oskin (Poster 151); Hearn et al. (Poster #152)

RHEOL_GUI

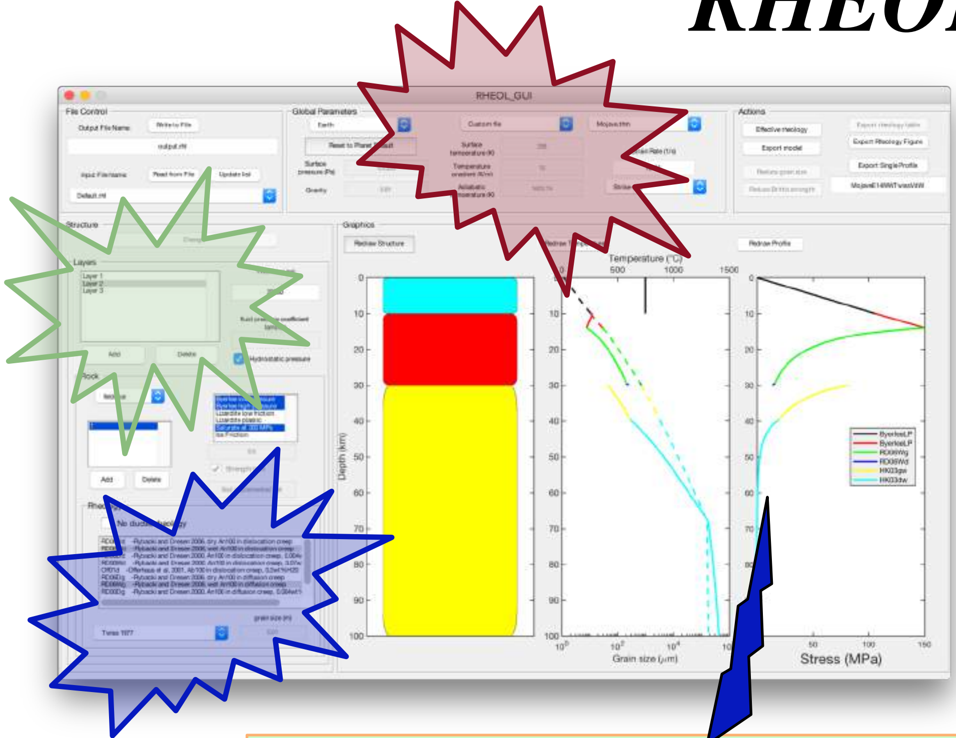

Select possible rheologies

Tempe-rature profile*

***From CTM**

Rock types*

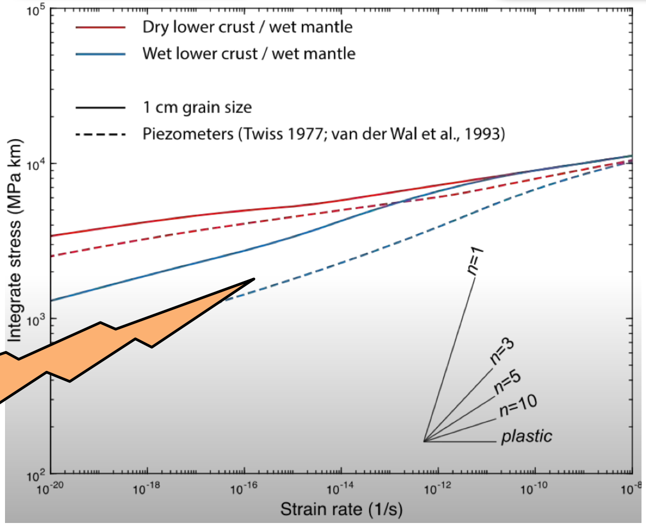

***From GF**

Build your own strength profile
And lithosphere-scale rheology!

Montési and Leete (Poster #150)
https://github.com/montesi/RHEOL_GUI

BASIN Project: Basin Amplification Seismic INvestigation

Tracking the propagation of waves from the San Andreas Fault to Los Angeles

Poster #099

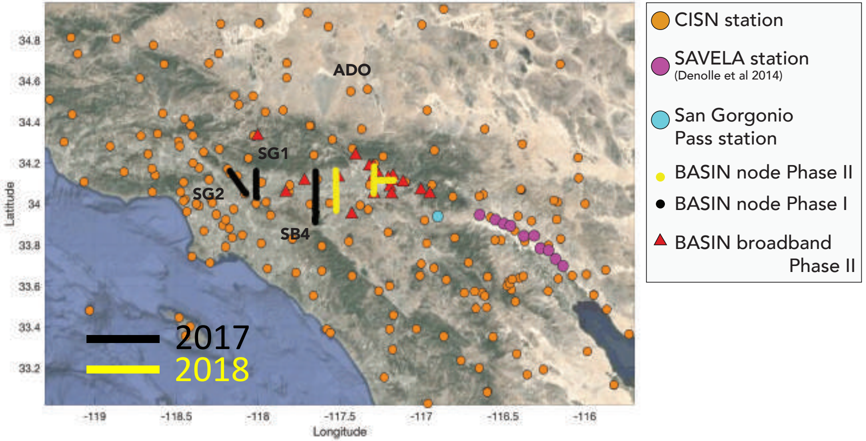

Robert Clayton, Caltech
Marine Denolle, Harvard
Kim Olsen, SDSU
Patricia Persaud, LSU
Jascha Polet, Cal Poly Pomona

Receiver Function Structure, Liu et al, Poster 276

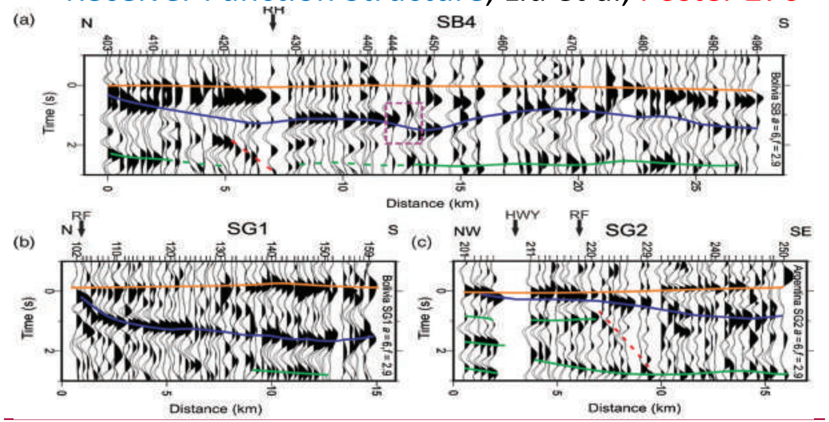

Site Response, Tayagi et al, Poster 111

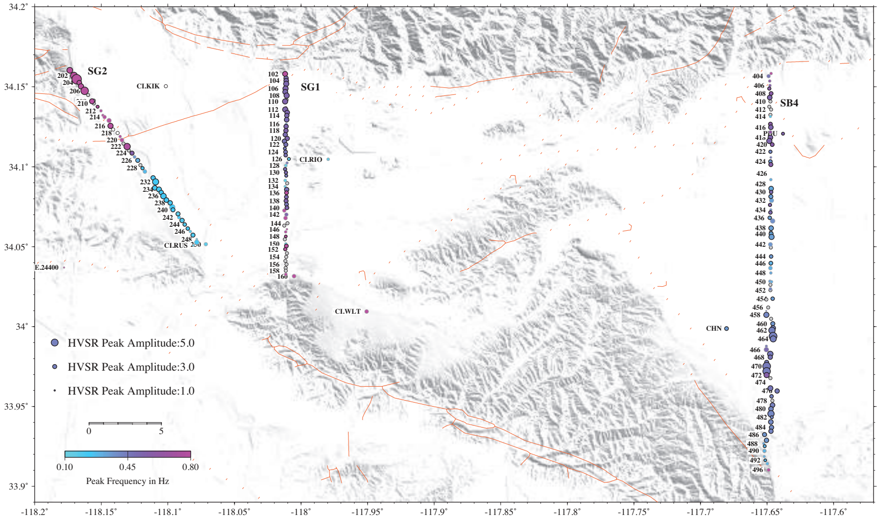

SC/EC

A Proposal for Industry-Scale Seismic Survey in the LA Basin

Southern California Earthquake Center

- 4,500 1C nodes rolled across 17,000 locations (30 days/station)
- 200 3C nodes static (120 days/station)
- 60+ deep hole shots

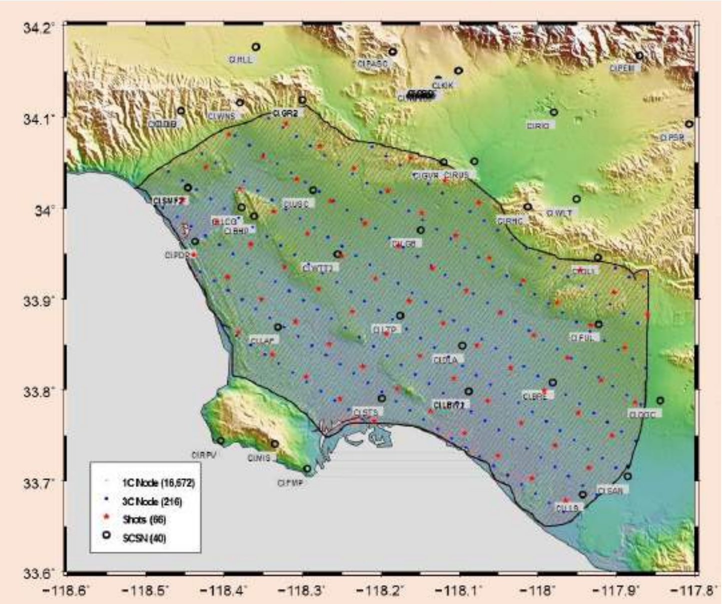

Hollis & Clayton (Poster #097)

Analyses

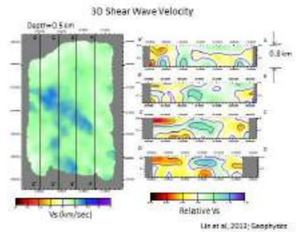

Lin, Fan-Chi, D. Li, R. Clayton, D. Hollis, 2013, High-resolution shallow crustal structure in Long Beach, California: application of ambient noise tomography on a dense seismic array, Geophysics, 78(4), Q45-Q56, doi:10.1190/geo2012-0453.1

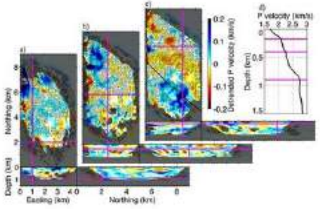

Nakata, N., J. Chang, J. Lawrence, P. Boue, 2015, Body wave extraction and tomography at Long Beach, California, with ambient noise interferometry, JGR, 120, 2,doi:10.1002/2015JB011870

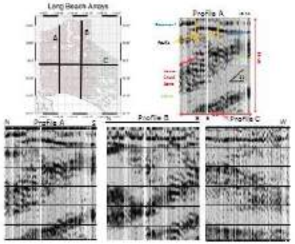

Clayton, R., 2018, Imaging the subsurface with ambient noise correlations", SEG2018 extended abstract

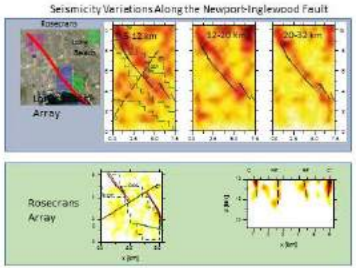

Inbal, A., J-P Ampuero, and R. Clayton, (2016) Localized Seismic Deformation in the Upper Mantle Revealed by Dense Arrays, Science, 354, pp88-92, doi:10.1126/science.aaf1370

Data Products

- 3D Basin Structure
- 3D Shear and Compression Velocity Structure
- Shallow Vs500, Vs1000 maps
- Active Structures
- And more…

Source → Path → Site Response

Differential noise interferometry kernels

Non-isotropic azimuthal noise intensity distribution

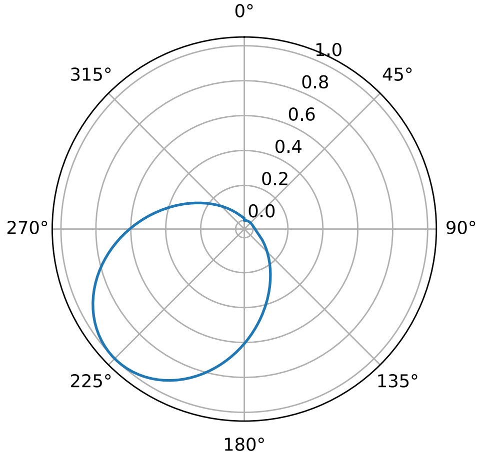

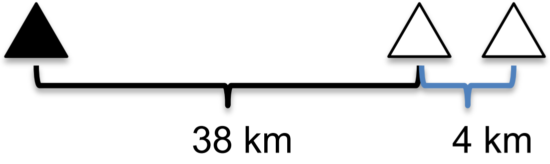

Travel time kernel

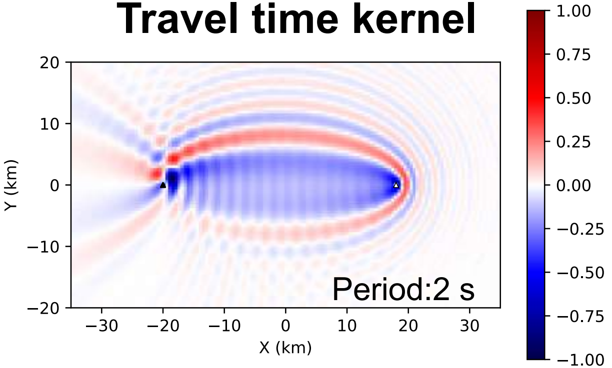

Amplitude kernel

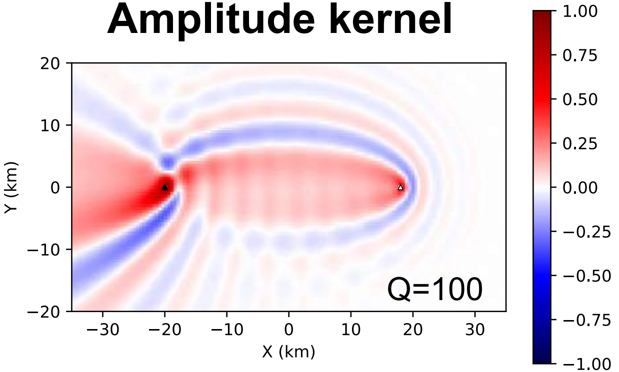

Differential travel time kernel

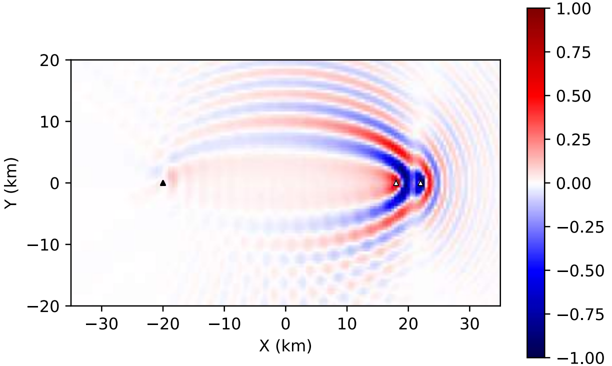

Differential amplitude kernel

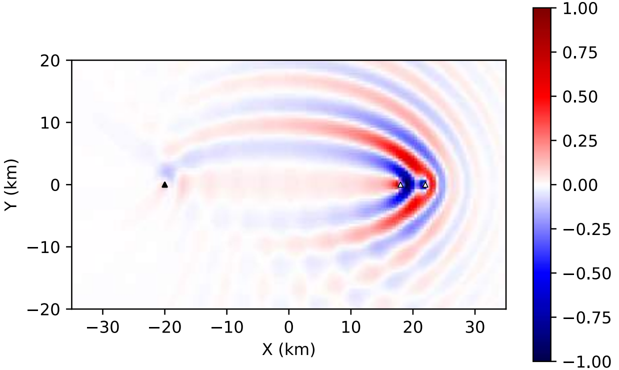

Liu & Beroza. (Poster #108)

Kernels of differential measurements reduce artifacts and bias

Consistency of CGM InSAR time series

Time series estimated using different approaches, different processing software, show good agreement with each other and with GPS

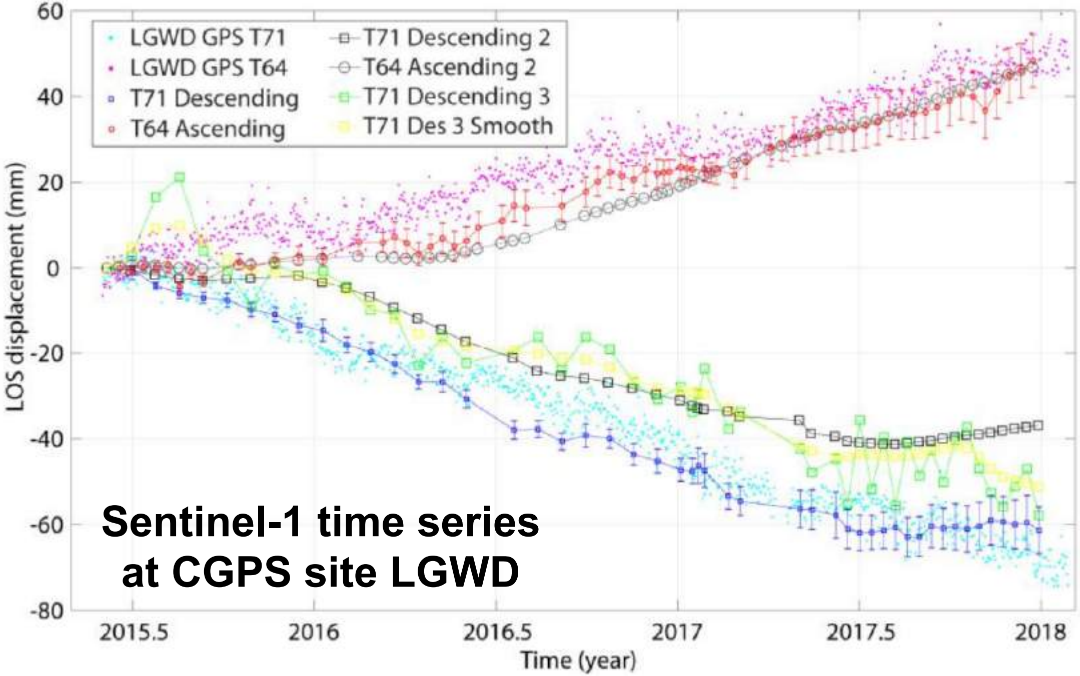

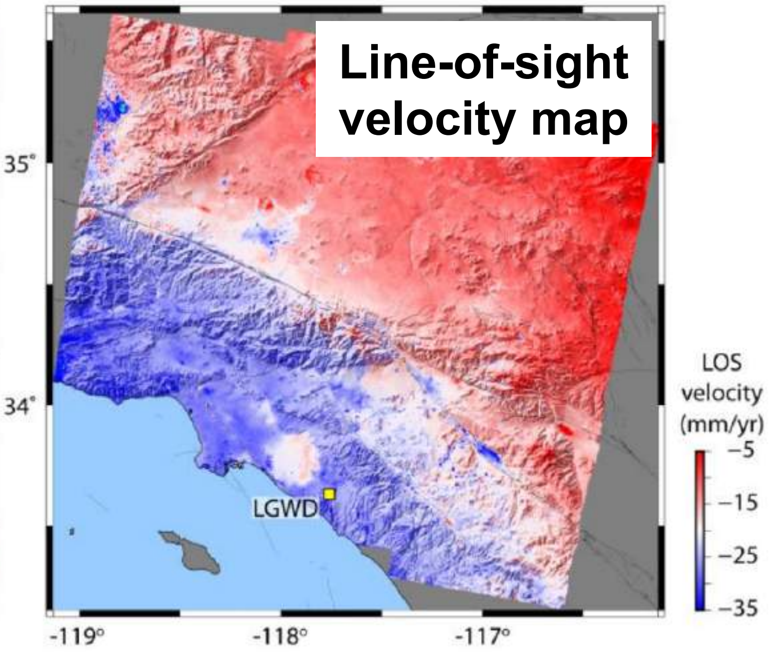

CGM InSAR working group (Figure: Xiaohua Xu)

4. Data-Intensive Computing

Similarity Matrix Profile (MP)

Efficient method to identify most similar sub-sequence in continuous data

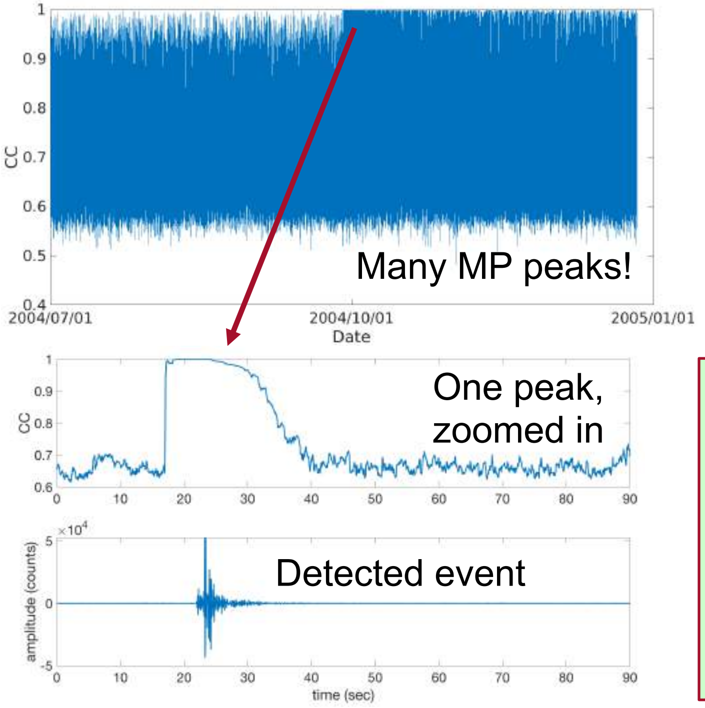

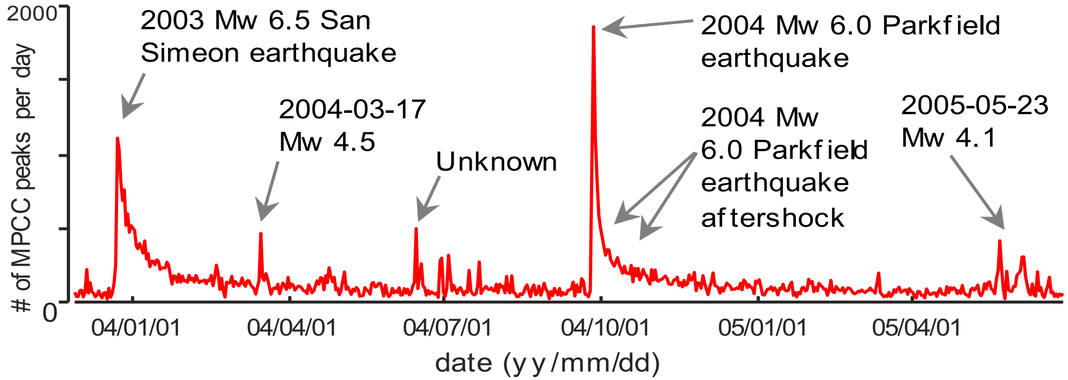

Using an AWS GPU cluster, the MP for 580 days (10^9 samples) of seismic data can be computed in ~10 hours!

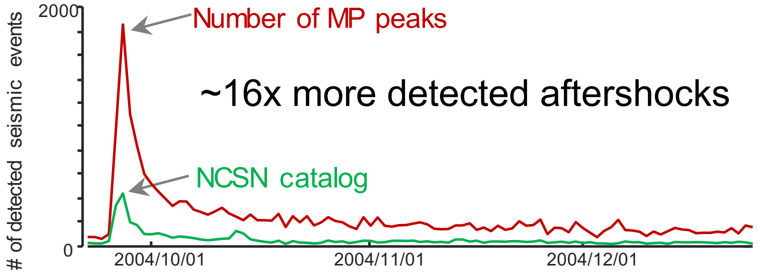

Shakibay Senobari et al. (Poster #063)

Characteristics of ground motion generated by interaction of wind gusts with trees, structures and other surface obstacles

Geophones targeting local vegetation and structures

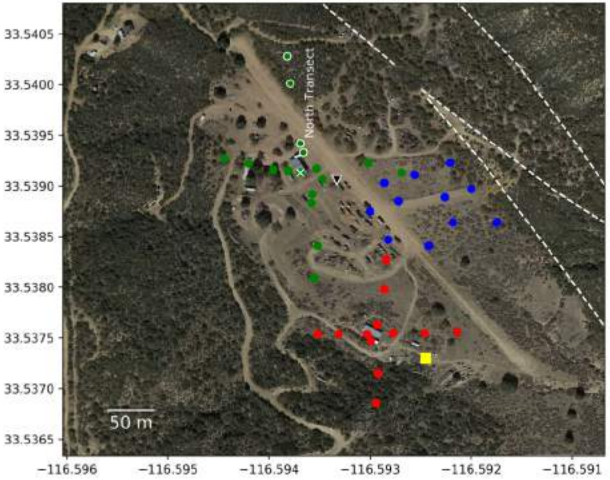

Waveforms originating from surface structure

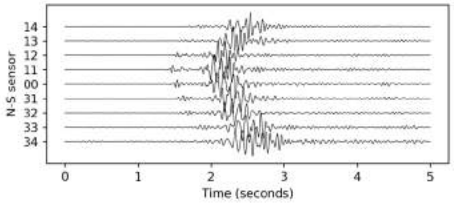

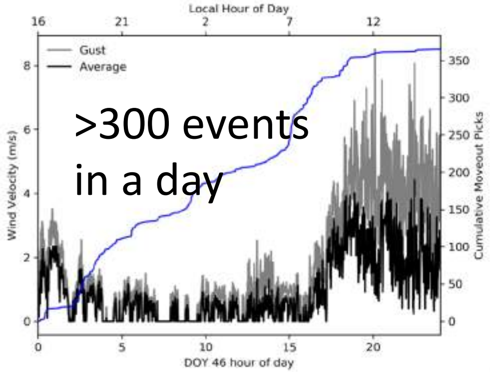

Wind & temp with borehole seismometer spectrogram

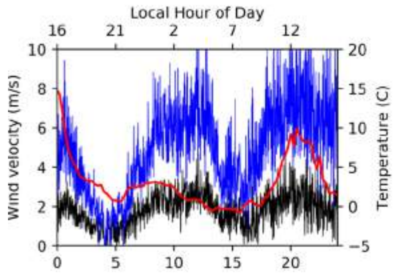

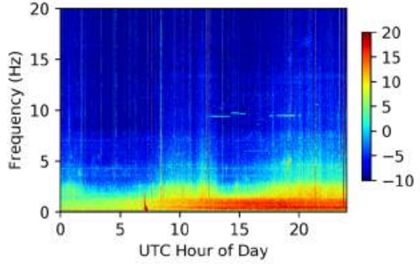

Johnson, C.W. et al. (Poster #305)

Wind interacting with surface structures, trees, etc. can mask microseismicity
Some of these surface interactions are observable at 150 m depth from 1-8 Hz

Generalized Seismic Phase Detection (GPD)

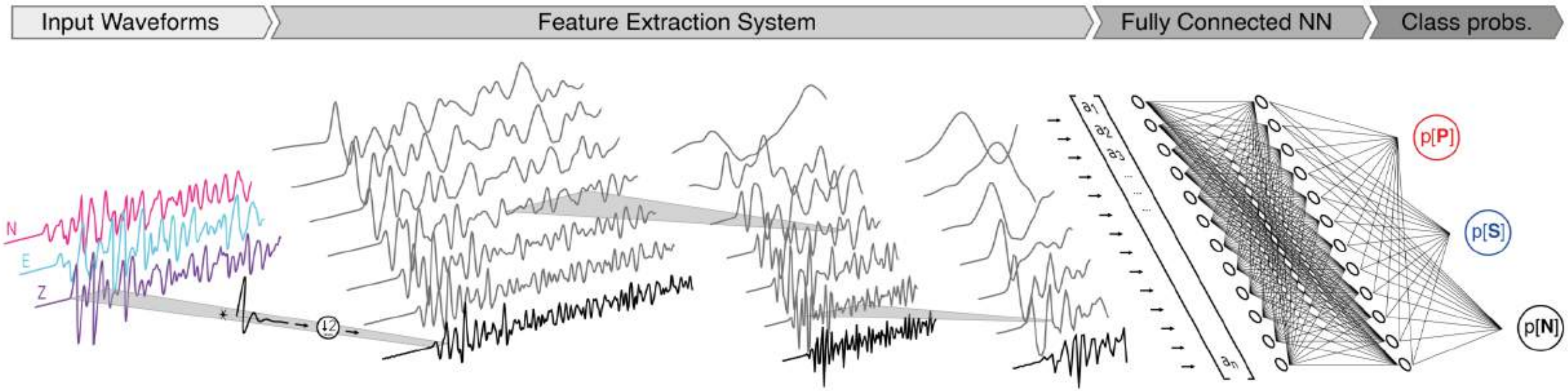

- Train a Convolutional Neural Network classifier with millions of labeled example waveforms
- Can reliably recognize i) P-waves, ii) S-waves, iii) ambient and impulsive noise signals
- Has similar sensitivity as template matching, but does not need explicit templates

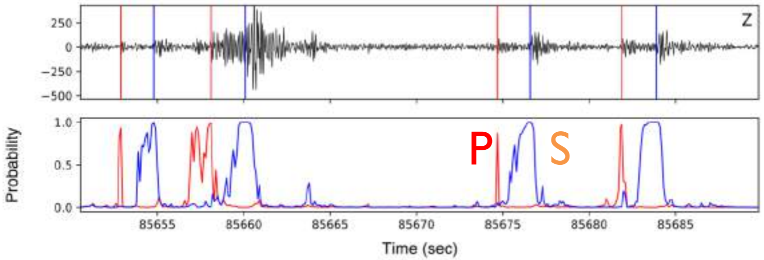

Meier et al. (Poster #064) / Ross et al., 2018, BSSA

Characterization of High-Wavenumber Subsurface Random Heterogeneity Using a Very Dense Array at Diablo Canyon, California

Receiver geometry

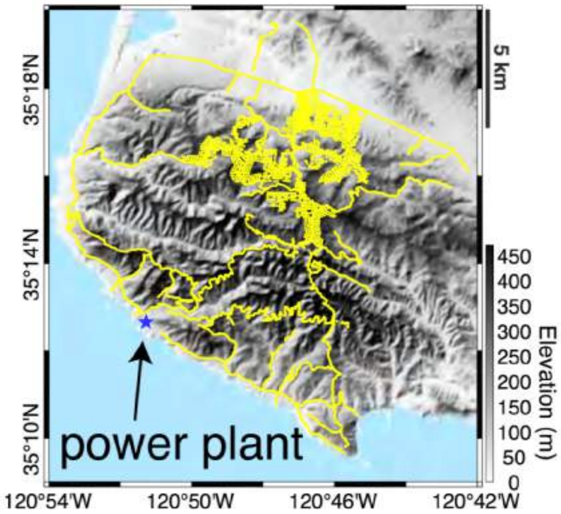

- 7200 v-comp geophones
- 10 Hz
- ~20 x 20 km^2
- Total 1.5 months recording

Ambient-noise correlation

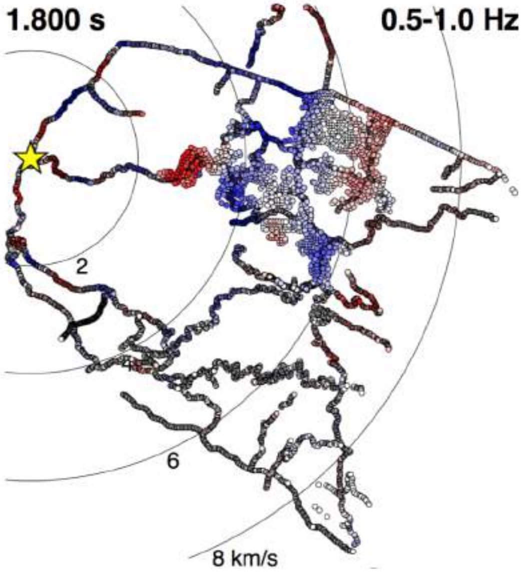

Coherent waves are extracted by correlation techniques.

Rayleigh-wave group velocity map

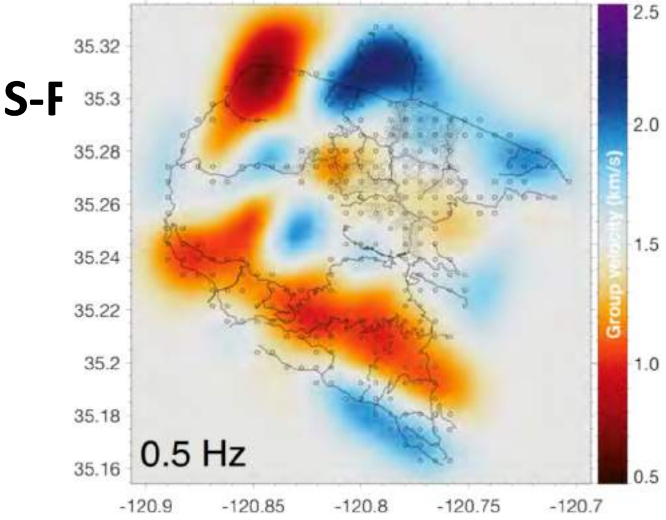

We can estimate detailed heterogeneity of the subsurface structure.

Very Dense Array is key to estimating subsurface structure with high resolution.

Nori Nakata (Poster #298)

Machine learning applied to tomography

- Ambient noise tomography on the Long Beach array (5200 geophones in 10x7km area).
- Higher resolution than conventional (e.g., Eikonal) tomography.
- The seismic image consists of pixels and patches.
- No training data required.

Machine learning inversion

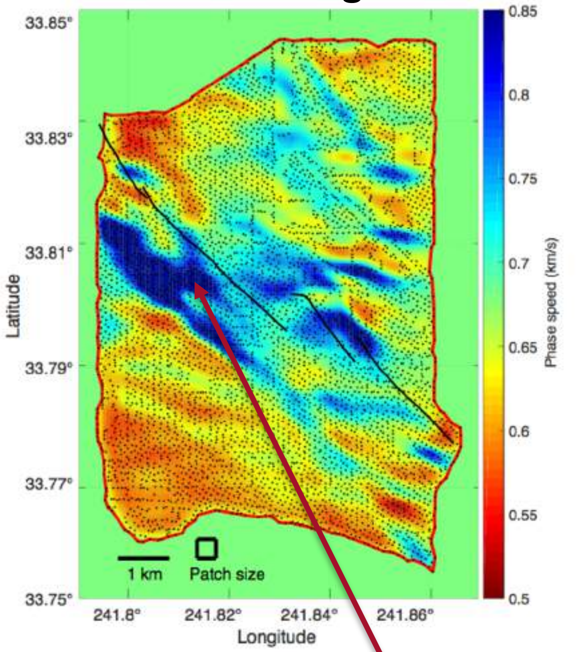

Conventional (Eikonal) tomography

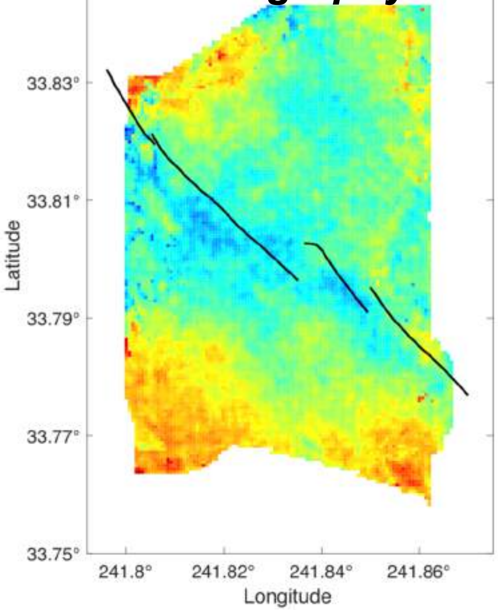

Bianco, Gerstoft, Olsen, Lin (poster #94)

High-velocity anomaly appears to be the main producing aquifer in Long Beach).

Physics Constrained Deep Neural Networks (PCDNN)

1. A toy model for frictional sliding with earthquake-like statistics

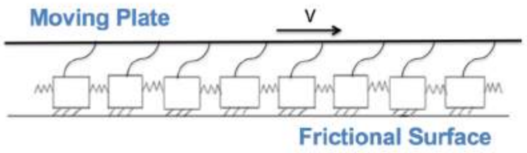

2. Multivariate LSTM Model Setup

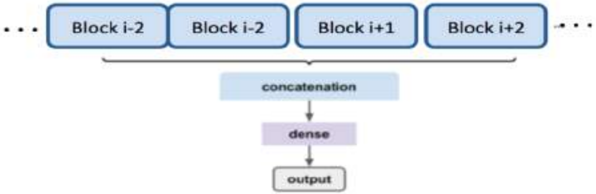

3. Training and Testing Dataset for block displacement time history

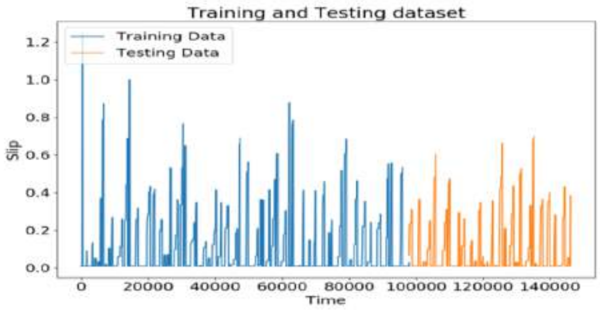

4. Single Feature LSTM VS Multivariate Feature LSTM Prediction

a. Single Feature LSTM

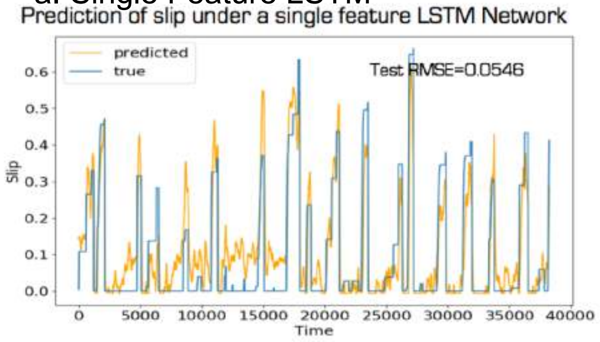

b. Multivariate Feature LSTM

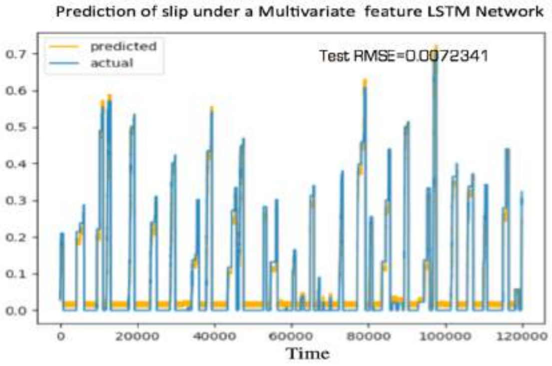

Physics-constrained deep learning networks encode the characteristics of spatial and temporal derivatives in governing PDEs by combining Convolutional Neural Networks (CNN) and Long Short Term Memory (LSTM) Networks.

By using constraints of the PDE structure, PCDNN uses less data in training, and its prediction outperforms traditional time series prediction using single feature LSTM or Poisson's processes.

This framework may improve earthquake forecasting and may significantly speed up forward computation as well.

Elbanna et al. Poster 199

Analysis of offset stream channels with very high resolution UAV imagery Southernmost San Andreas Fault

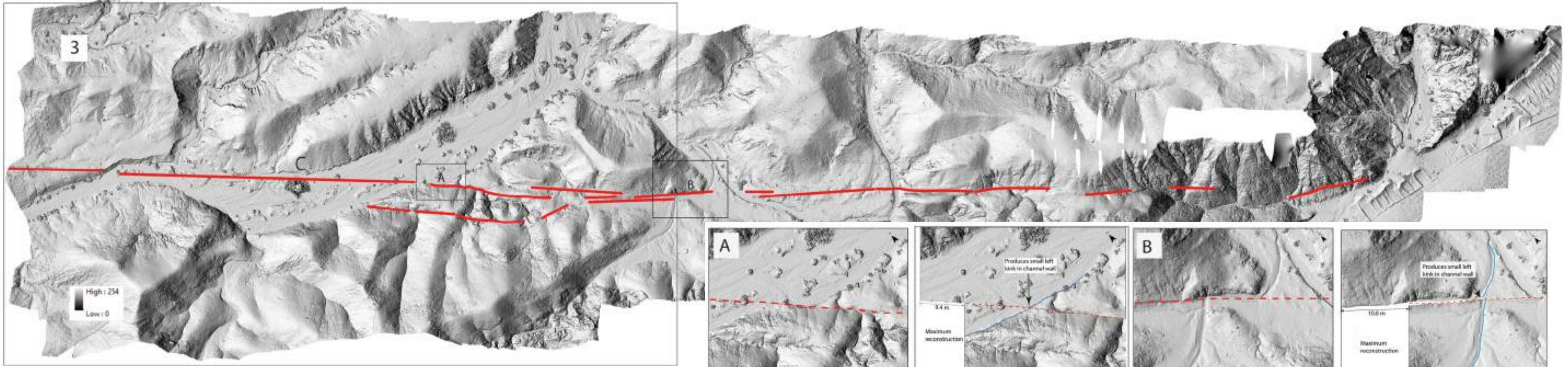

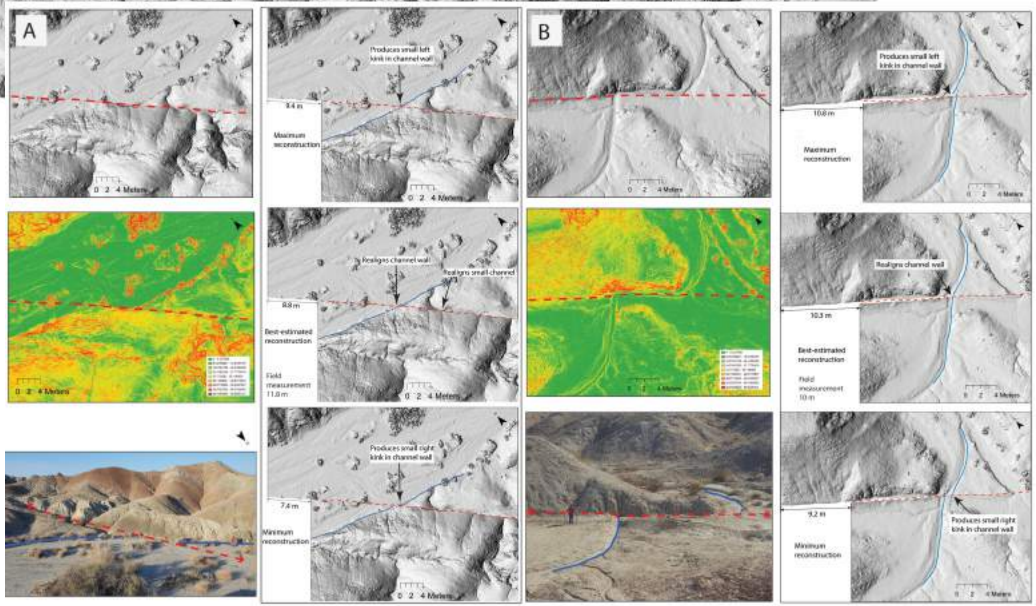

Sub-centimeter pixel resolution

Many small and large displacements ranging from 50 cm (creep) to 100 m

These 2 examples are offset 9-10 m

Blanton et al. (Poster #226)

Earthquake Simulations on Deep Learning Hardware

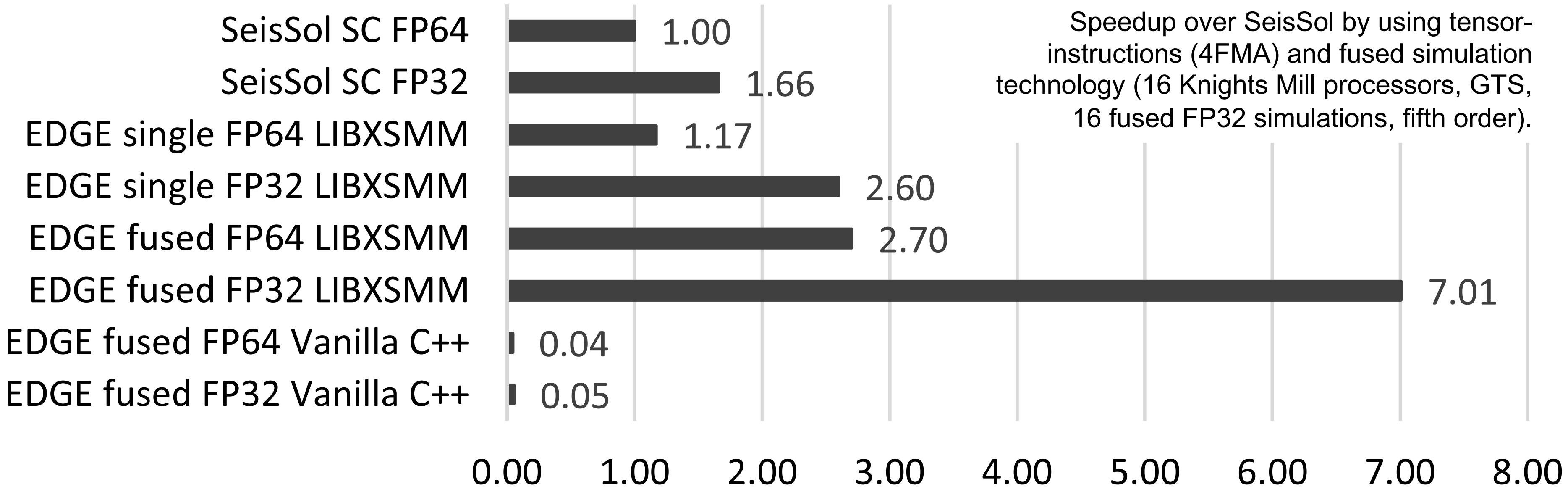

Speedup over SeisSol by using tensor-instructions (4FMA) and fused simulation technology (16 Knights Mill processors, GTS, 16 fused FP32 simulations, fifth order).

Achieved efficient HPC utilization of the Intel Xeon Phi for Deep Learning.

Breuer et al. (Poster #289)

Theme B. Understanding Earthquake Processes

5. Beyond Elasticity
6. Modeling Earthquake Source Processes
7. Ground Motion Simulation
8. Induced Seismicity

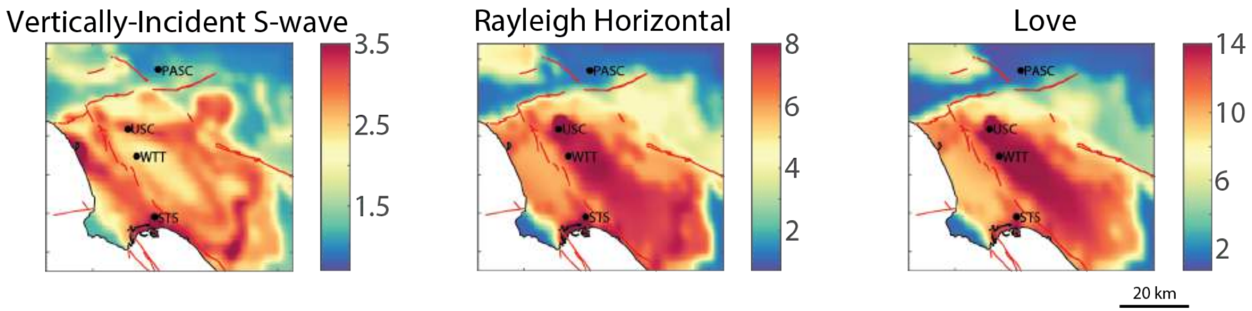

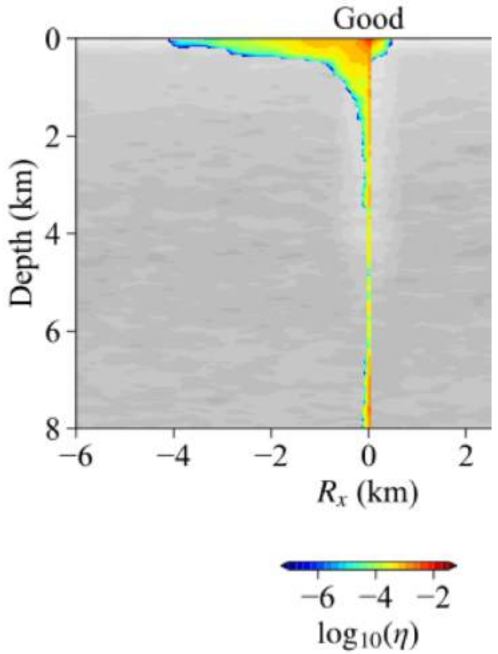

5. Beyond Elasticity

Large Scale: Rock damage production in southern California

Damage volume, 1981-2017

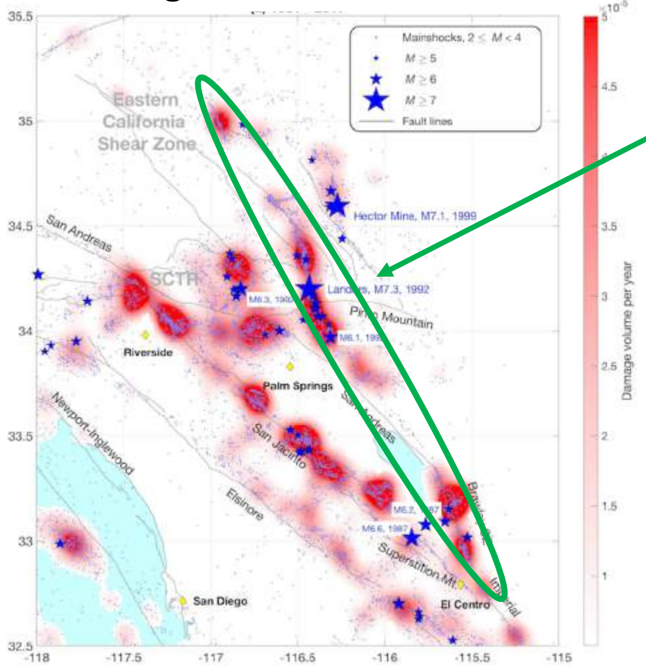

Damage volume, 1981-1990

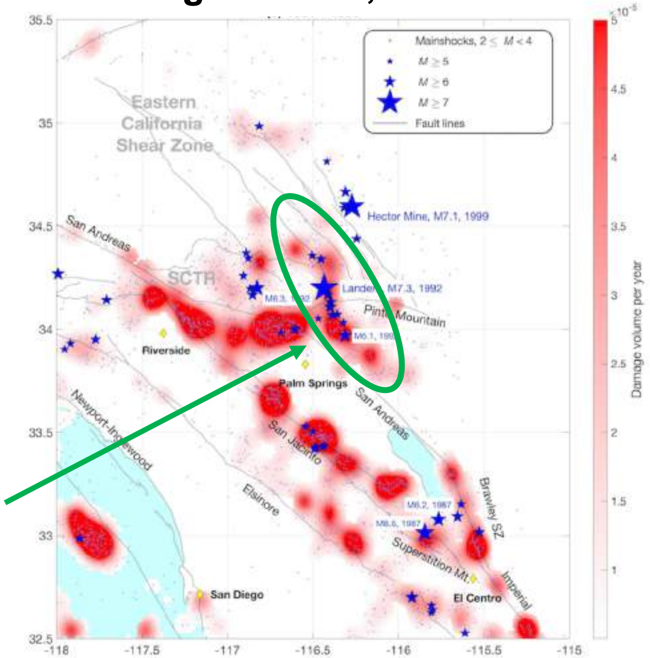

A quasi-linear zone with ongoing damage production between the Imperial fault and ECSZ

The regions around the 1992 Joshua Tree, Landers and Big Bear events have background seismic activity before 1990

Ben-Zion & Zaliapin (Poster #066)

Intermediate Scale: High-resolution fault imaging

DDT = double-difference tomography
FZHW = fault zone head waves

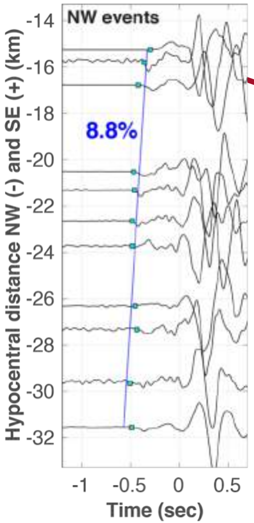

FZHW along northern SJF

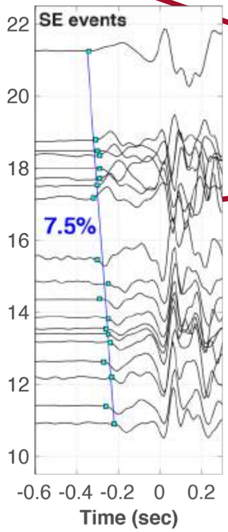

DDT model

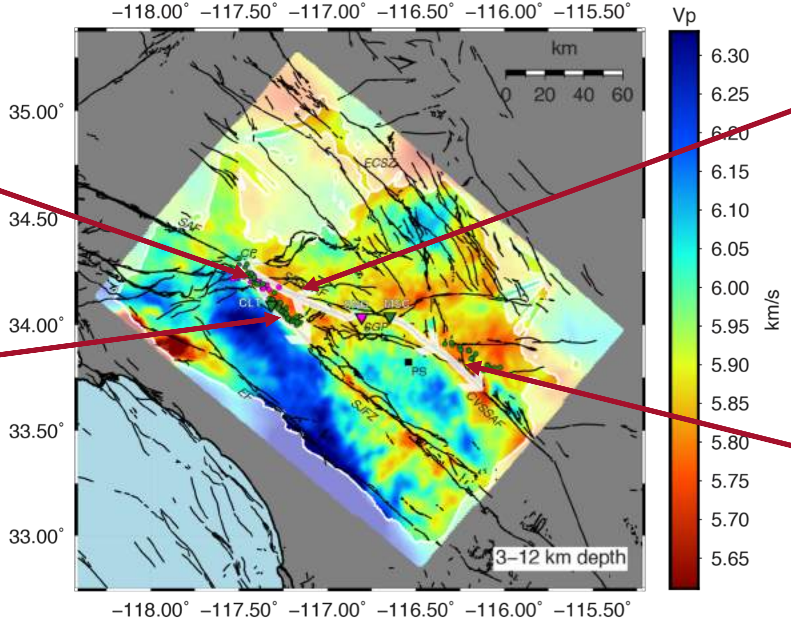

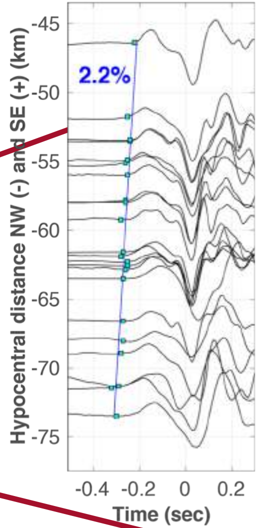

FZHW along SAF

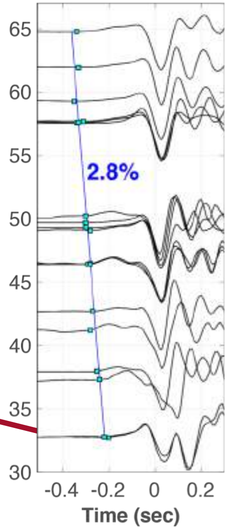

Implications of imaging results:

SAF earthquakes likely propagate to the NW and SE from San Gorgonio Pass.
Rupture on the Mojave SAF can easily trigger continuing rupture on the SJF.
NW rupture on the SJF not likely to trigger continuing rupture on the SAF.

Share et al. (Poster #101)

Small Scale: Microstructural and microchemical analyses of active faults

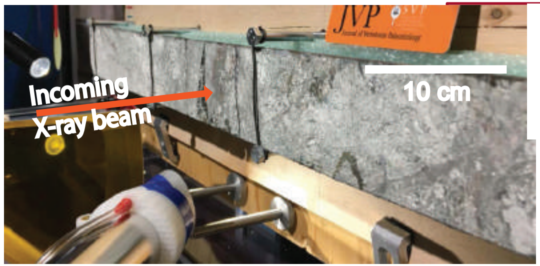

High energy X-ray mapping at the Stanford Synchrotron Lightsource for geochemical analyses of San Andreas at Lake Elizabeth ***Core at Lake Elizabeth (Edwards et al., 2018).***

Lots of energy goes into chemical alteration and distributed damage.

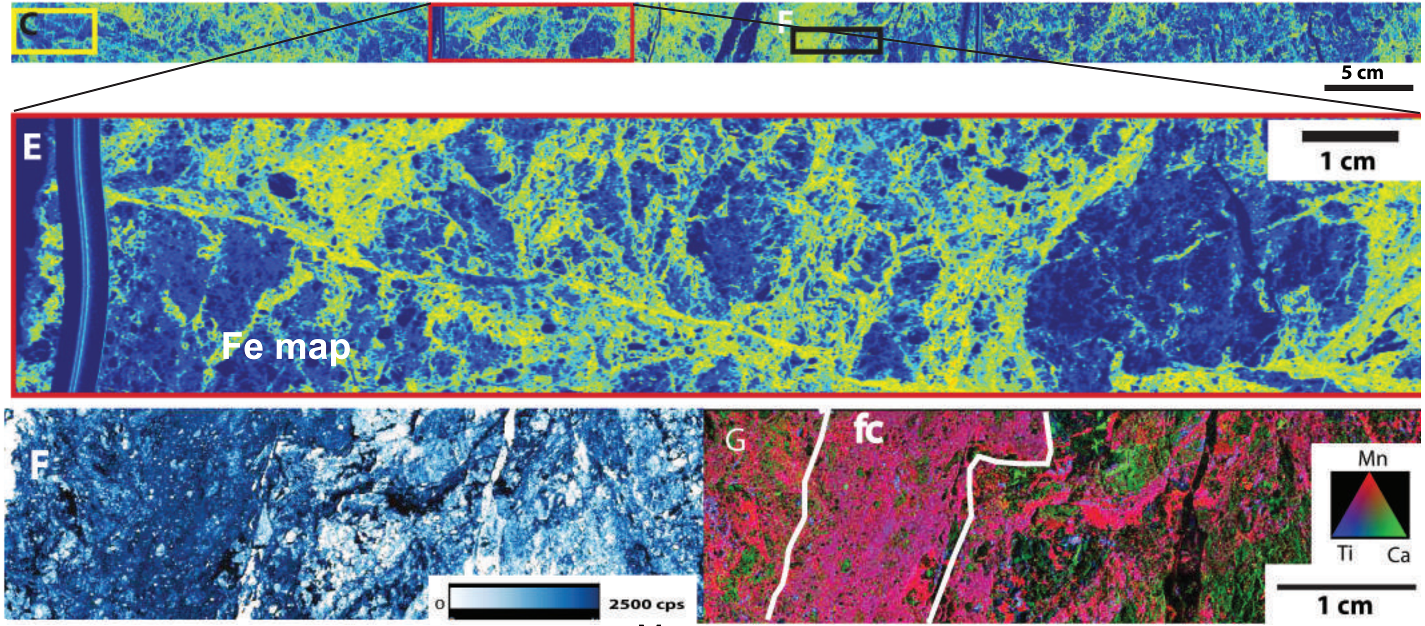

Mn map

Ca-Mn-Ti map

8 cm

Evans et al. (Poster #169)

How does inherited structure and fabric control fault loading?

Width of shear zones and fault loading mechanism?

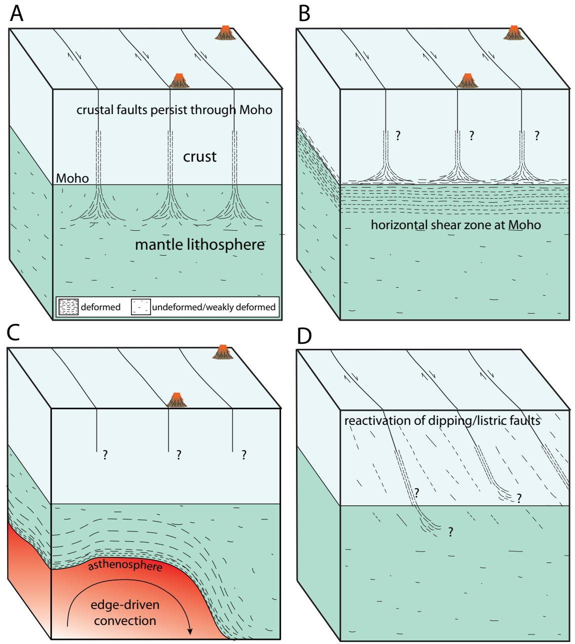

New, dense broadband deployment across ECSZ faults to infer structure

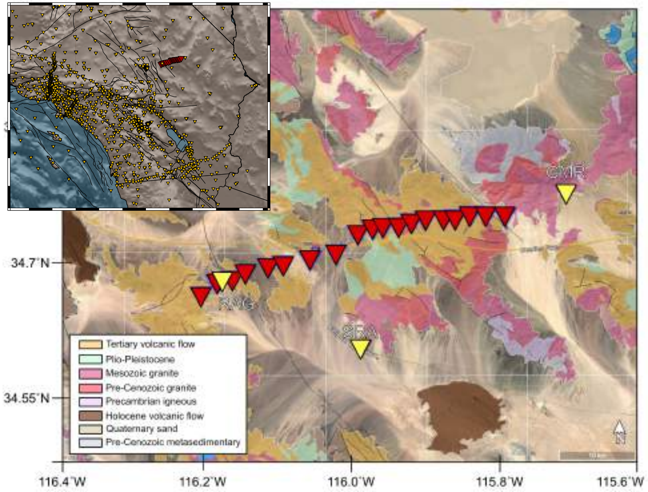

Evidence for fabric at depth

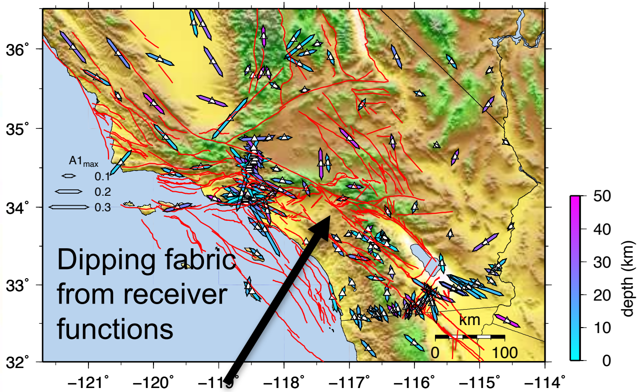

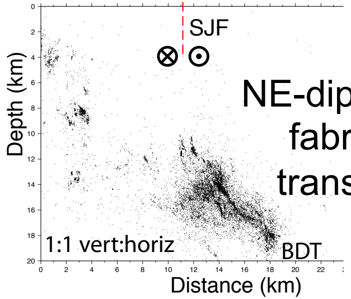

NE-dipping regional fabric, dipping transform faults

Becker et al. (Poster #157)
Schulte-Pelkum et al. (#159)

Fault/shear fabric reactivation results in non-optimal orientations (dipping strike-slip); anisotropic rheology?

6. Modeling Earthquake Source Processes

SCEC Initiative on Comparing Simulations of Earthquake Sequences and Aseismic Slip (SEAS)

- **Led by Junle Jiang and Brittany Erickson**
- **First workshop on April 23-24, 2018 in Pomona, jointly w/ dynamic rupture group.**
- 60 participants from 7 countries (half students/postdocs); 11 modelers in first SEAS benchmark.
- **First SEAS benchmark: 2D elastic, quasi-dynamic, planar fault, rate-and-state friction**

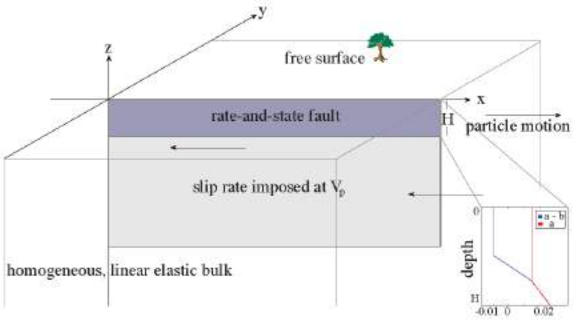

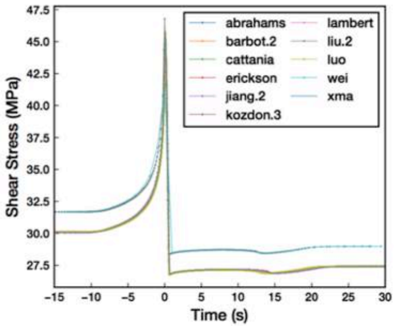

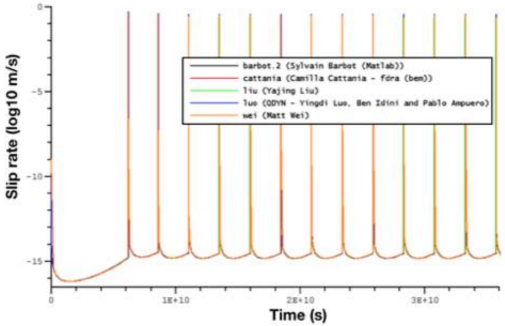

- **SCEC talk on Monday 14:00, corresponding poster #192.**
- **Future SEAS benchmarks to include:**
  - Fully dynamic earthquake sequences, coupling with fluids, involving multiple fault segments and nonplanar fault geometries, material heterogeneities, and bulk inelasticity.

- **Objectives**: provide community tools for best practices, move towards validating models with data.

Mechanisms of Unsteady Shallow Creep on Major Crustal Faults

Why do spontaneous/triggered shallow creep events occur on some crustal faults, such as the Southern San Andreas fault, Superstition Hills fault, and North Anatolian fault?

Jiang and Fialko (Poster #188)

- Explore depth-dependent fault conditions promoting episodic creep
- Construct long-term fault slip history from seismic-cycle observations

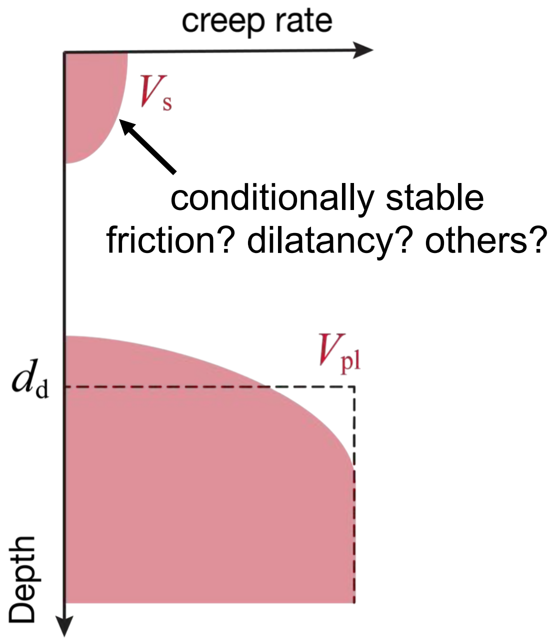

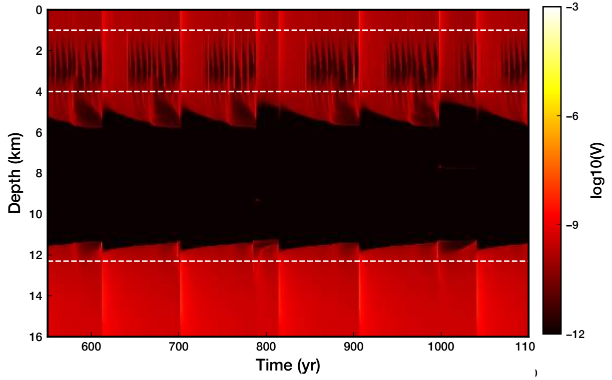

time evolution of slip rate

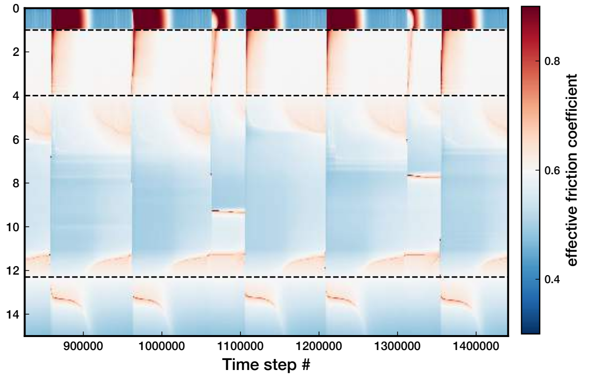

time evolution of friction

Dynamic strengthening processes are likely important in controlling the seismic potential of these shallow fault zones

Kali Allison and Eric Dunham (Poster #161)

Shear Heating and the Brittle-Ductile Transition (BDT): Earthquake Cycle Simulations with Power-law Viscoelasticity and Thermomechanical Coupling

without shear heating

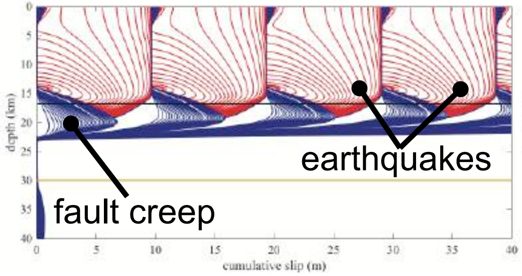

with shear heating

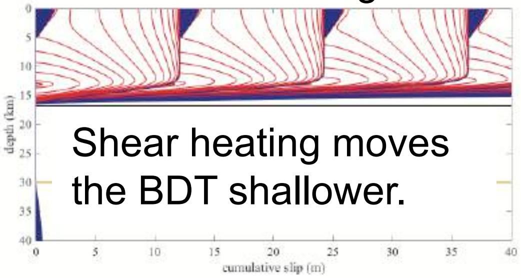

We investigate how pore pressure, background geotherm, and frictional shear zone size affect earthquake cycle characteristics and the depth of the BDT.

total thermal anomaly (difference from 1D geotherm)

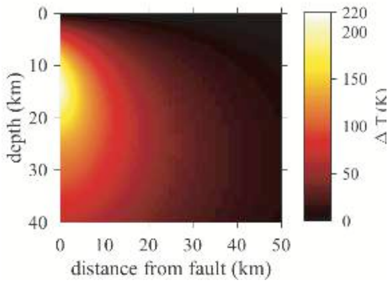

=

temperature rise from fault friction

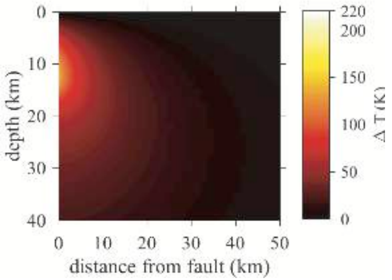

+

temperature rise from bulk viscous flow

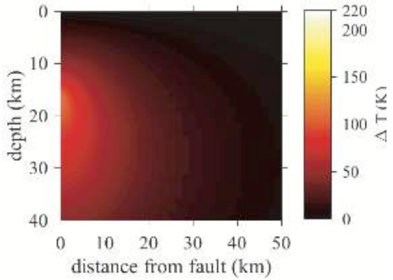

The contributions from frictional and viscous shear heating are roughly equal in magnitude.

A FEM-based Dynamic Earthquake Simulator for Geometrically Complex Faults with RSF

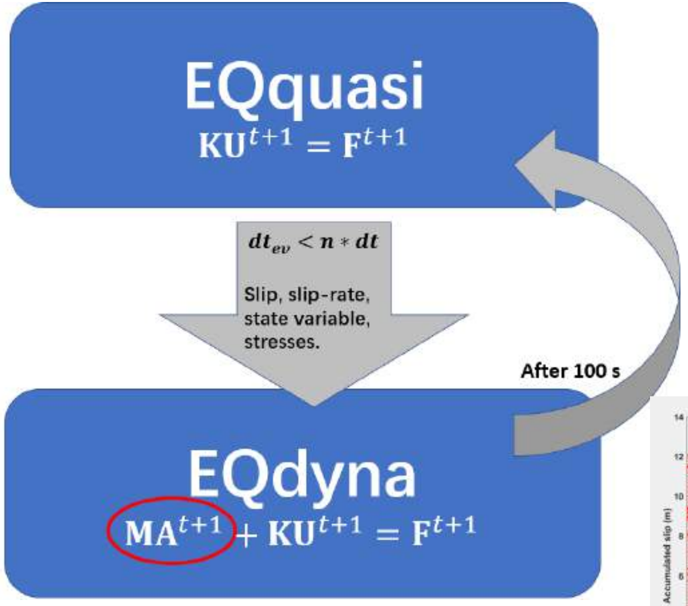

Based on the variable time stepping scheme (*Lapusta et al.*, 2000), the inertia term should be taken into account when the criterion is met.

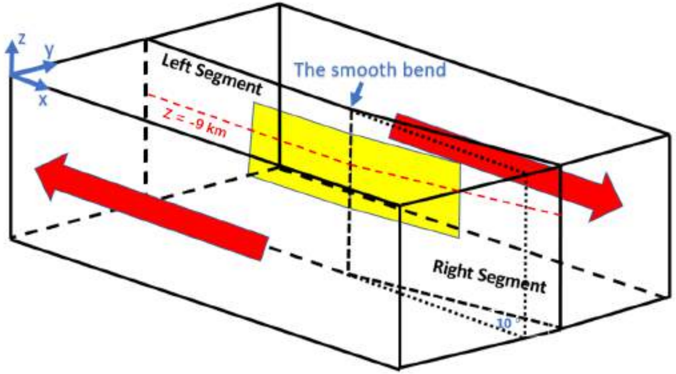

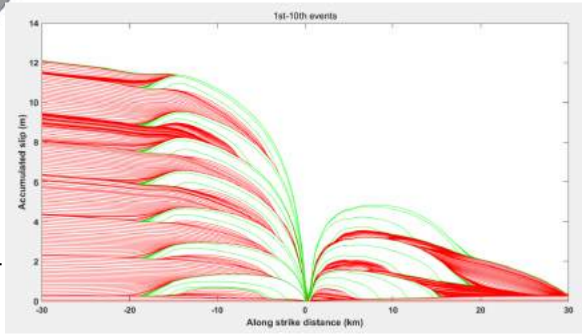

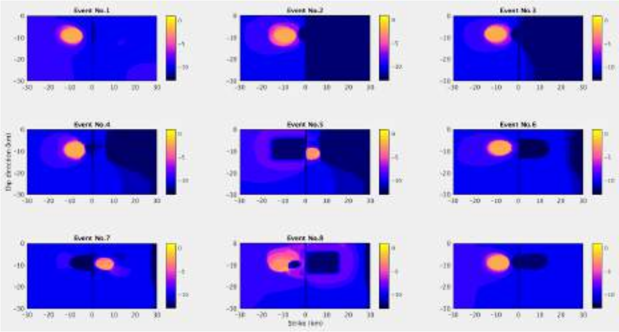

Liu et al. (Poster #205)

The FEM-based dynamic earthquake simulator makes fully dynamic EQ cycle simulations on geometrically complex faults possible

Crack models of repeating earthquakes

Numerical simulations:

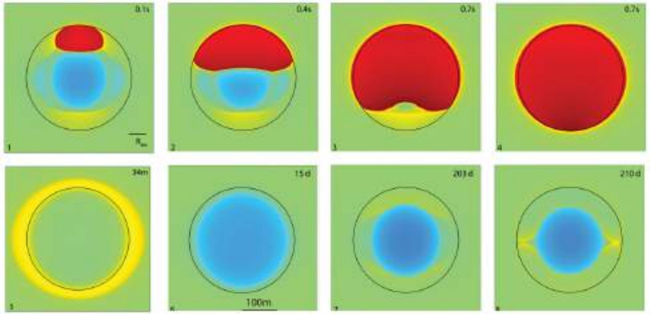

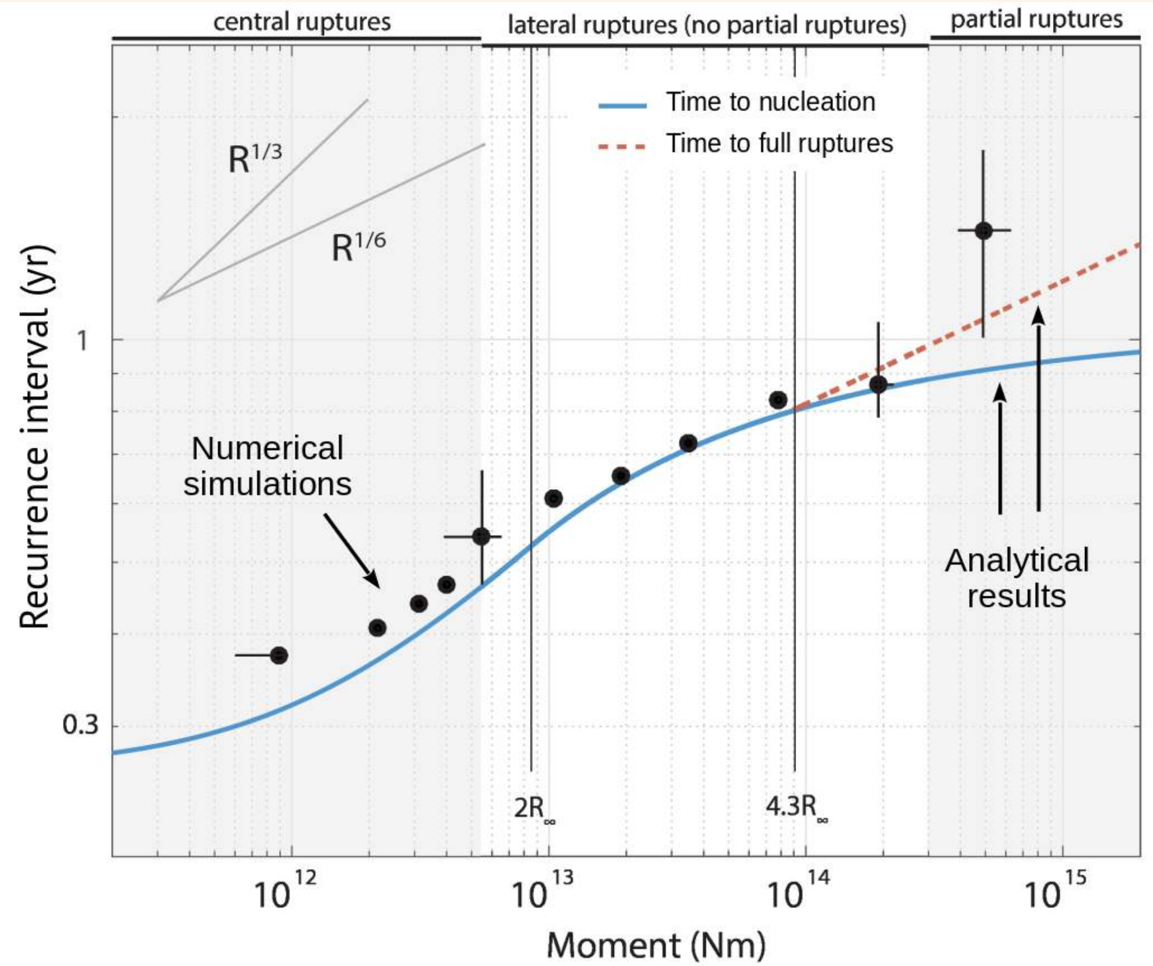

Analytical results explain the observed recurrence interval scaling of small repeating earthquakes ($Tr \sim M_0^{1/6}$)

Cattania and Segall (Poster #190)

Southern California Earthquake Center

Earthquake Source time functions

Sub-event analysis in source time functions

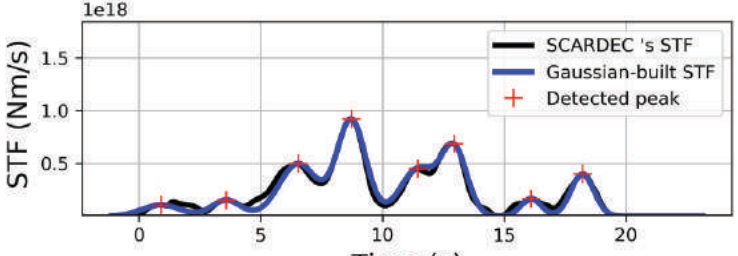

Estimating the magnitude before the earthquake stops

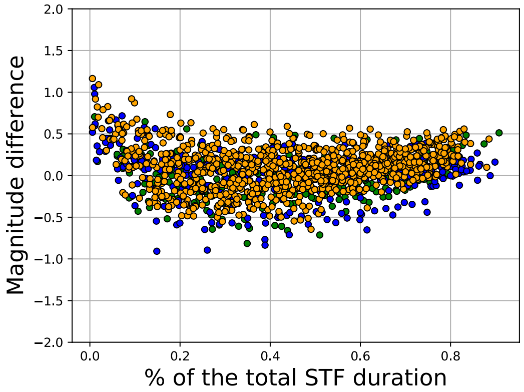

Sub-events scale with final earthquake size

Observations

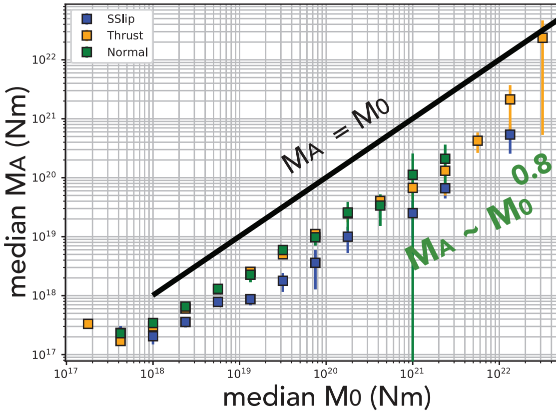

Simulations

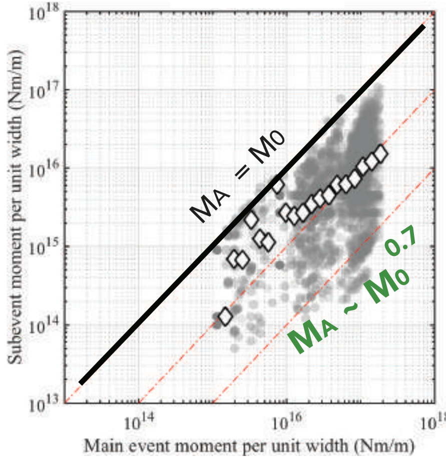

Specific and highly heterogeneous fault strength
Moderate earthquake rupture determinism

Danre et al., Denolle et al., (Posters #213, #214)

Faulty Intuition about b-values and Aftershock Productivity within a Fault Network

b-values appear to be lower near faults . . . . . . unless you define the faults *ahead of time*.

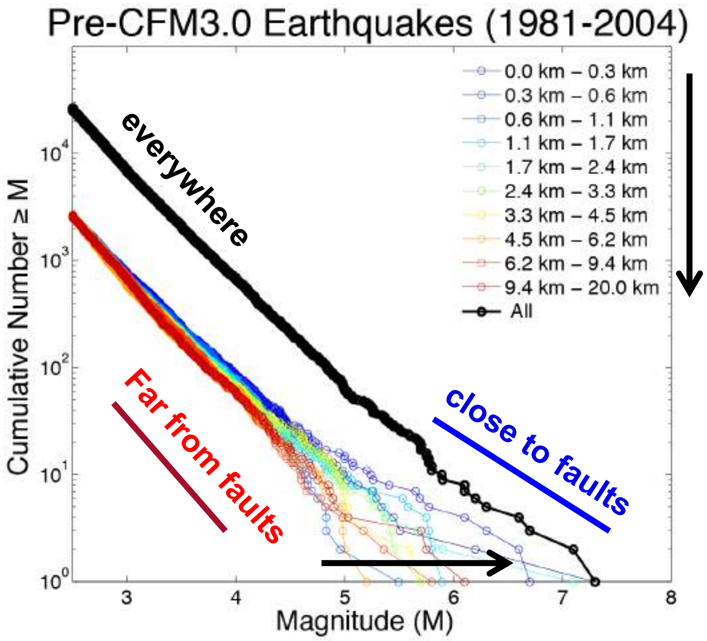

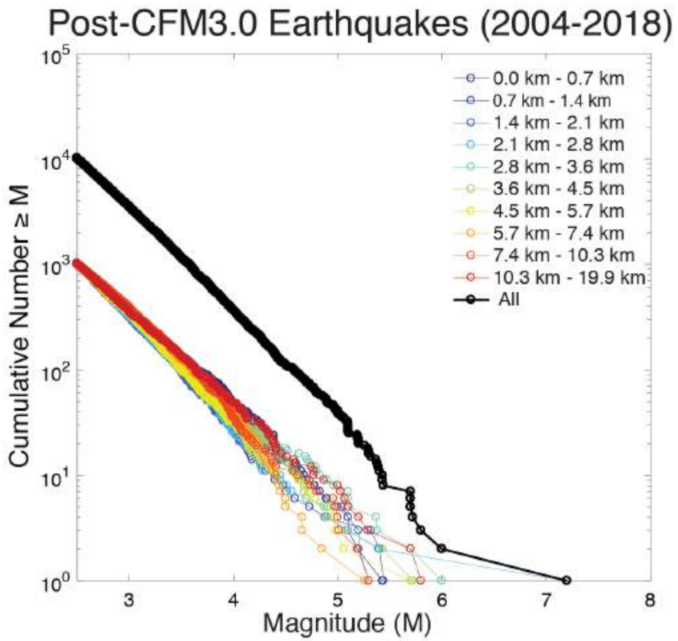

Suggests the CFM is overly tuned to past seismicity

Page & van der Elst (Poster #044)

8. Induced Seismicity

Injection Induced Earthquake Forecasting In Oklahoma

Southern California Earthquake Center

Zhai and Shirzaei, poster #35

Physics-based model of injection-fluid diffusion, Coulomb stress change and rate-state nucleation reproduces features of induced seismicity in OK.

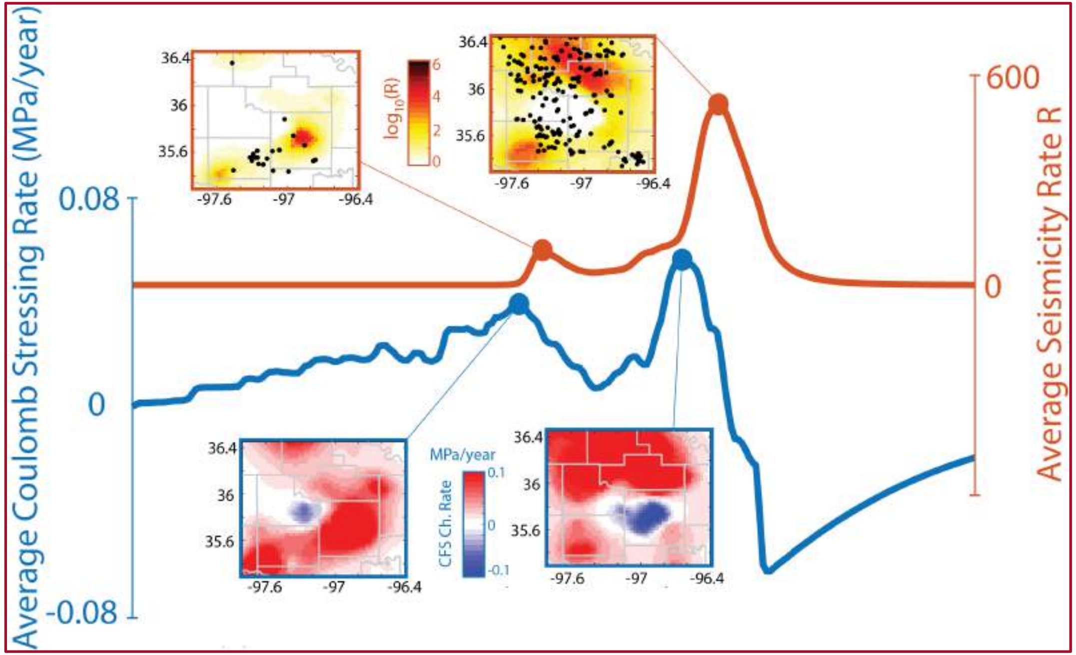

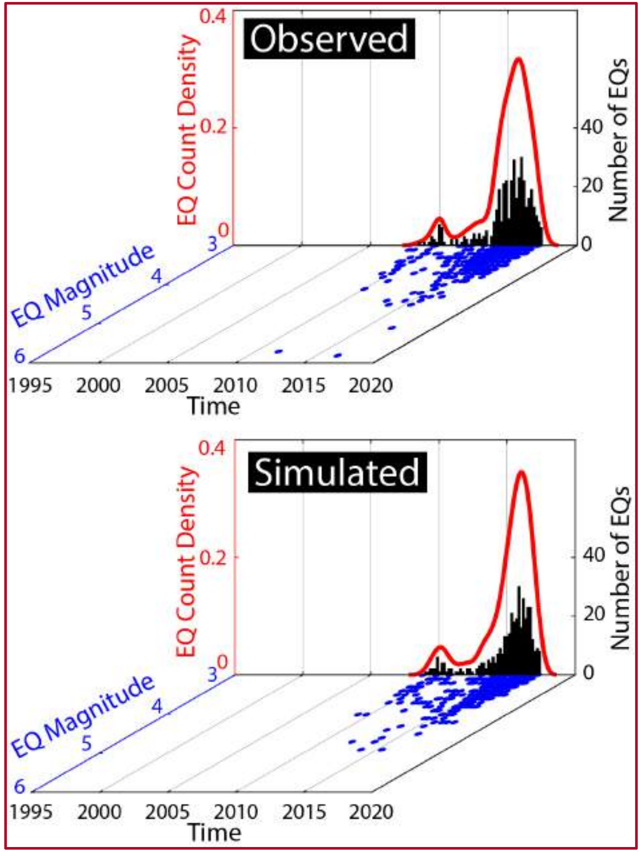

Induced seismicity mitigation and aftershock productivity in Oklahoma

T.H.W. Goebel[1], Z. Rosson[2], E.E. Brodsky[1], J. Walter[2]
1 UC Santa Cruz, 2 University of Oklahoma

Aftershock productivity

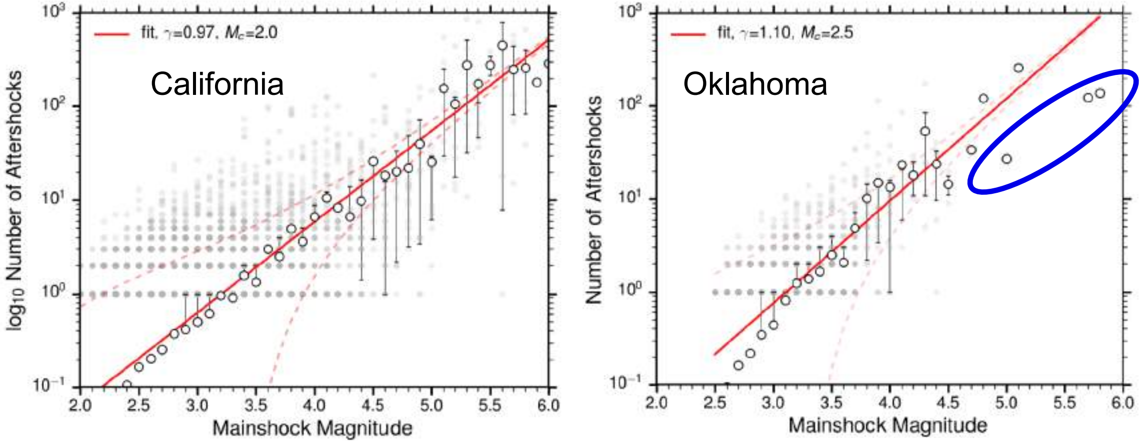

Low Productivity Events

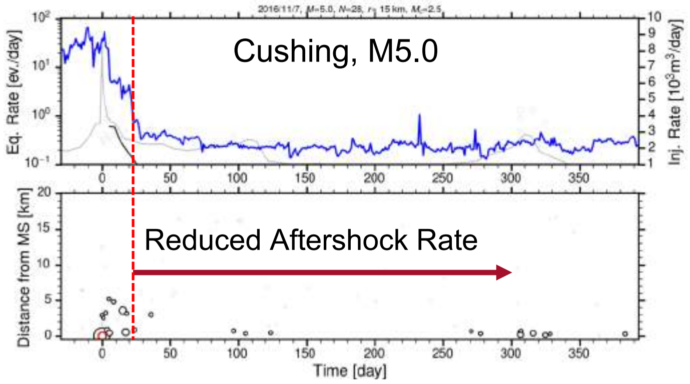

Aftershock productivity in Oklahoma is higher than in California. However, regions with active mitigation exhibit anomalously low productivity aftershock sequences.

Goebel et al. (Poster #089)

Modeling slip due to fluid injection into rate-and-state faults

Poster 186: Stacy Larochelle, Nadia Lapusta, Jean-Paul Ampuero, and Frédéric Cappa

Field experiment: **Aseismic slip** triggered by fluid injection + seismic later

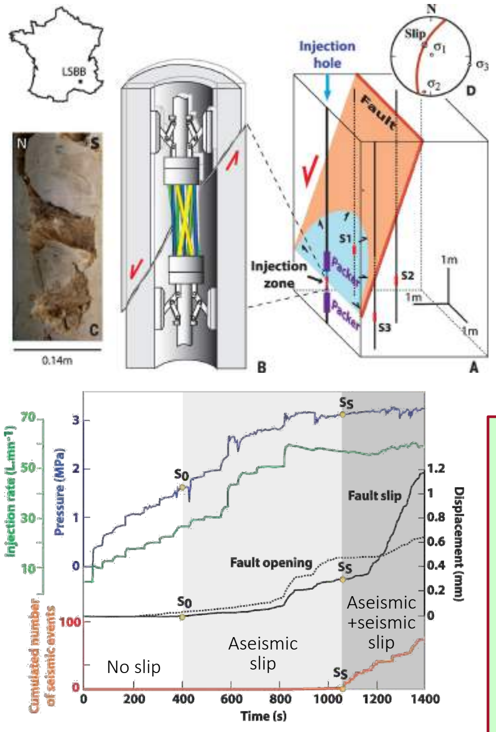

2D BICyclE code for **simulating fault slip** with along-fault fluid diffusion

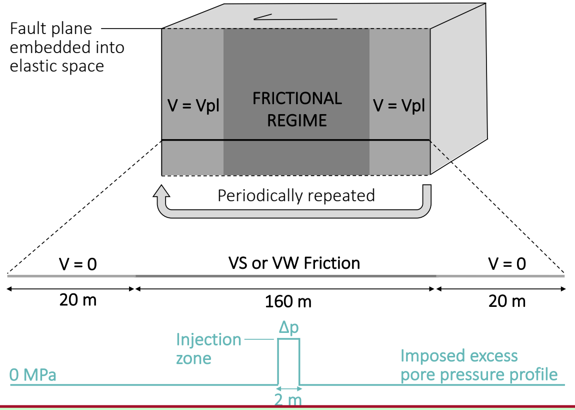

Injection-related measurements are insufficient to constrain friction properties.

Next step: use lab-measured friction to constrain coupling between slip & pore pressure evolution.

Initial aseismic fault slip Is well-reproduced by a range of fault properties

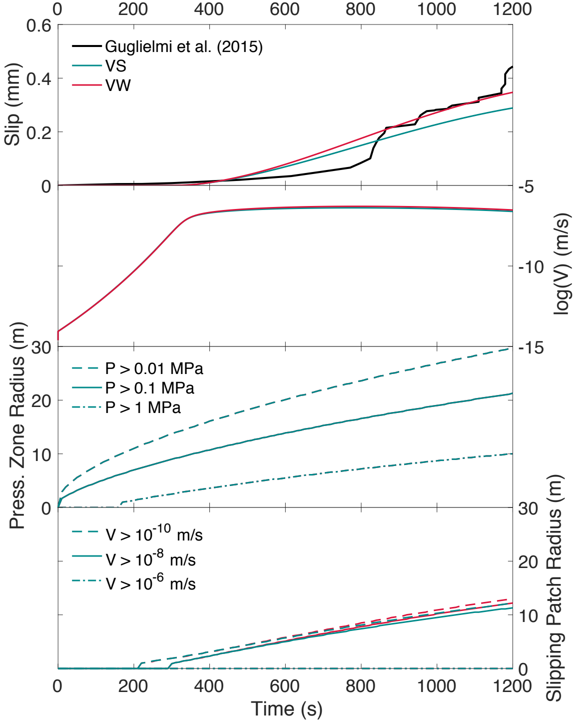

7. Ground Motion Simulation

Improved nonlinear High-F simulations

Surface displacement of elliptical basin: SV-incidence

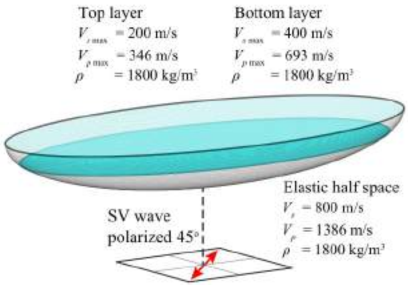

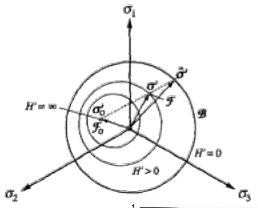

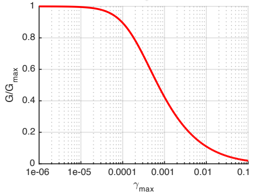

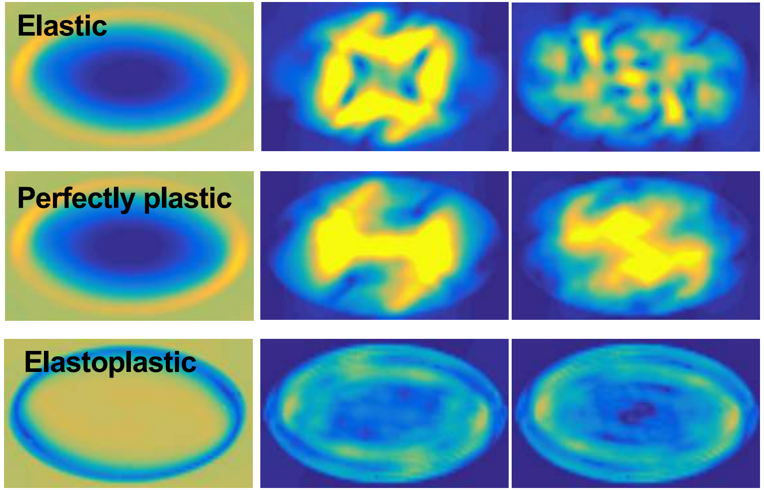

t = 2.5 sec t = 5 sec t = 7.5 sec

Elastoplastic: Borja-Amies bounding surface plasticity

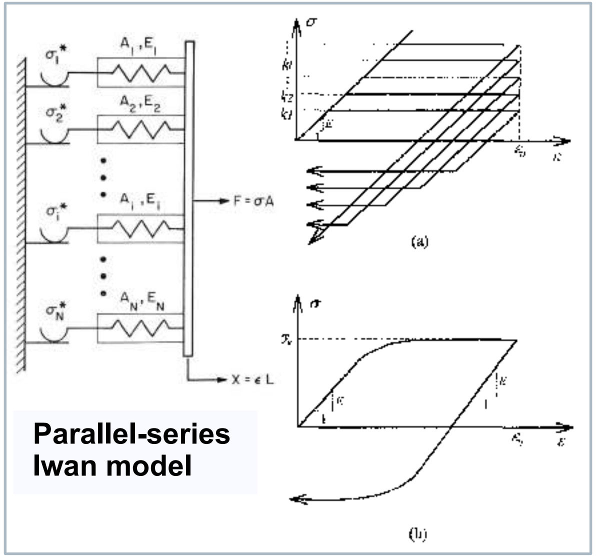

Roten et al. (Poster #019)

Esmaeilzadeh Seylabi et al. (Poster #020)

Beyond perfect plasticity: Elastoplastic 3D constitutive models for the shallow crust improving strong GM simulations

Higher resolution imaging techniques

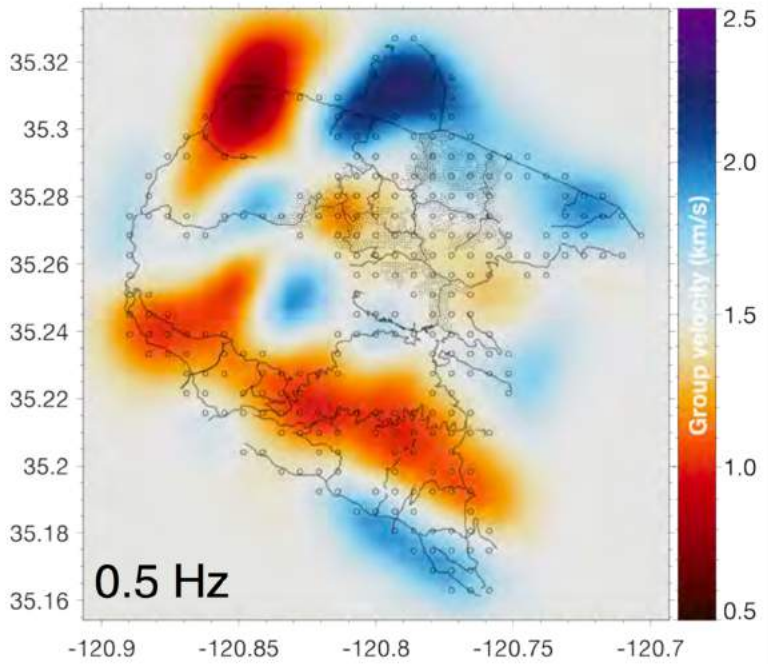

Group velocity inversion of noise correlation

Nakata (Poster #298)

Retailleau & Beroza (Poster #304)

Jia et al (Poster # 098) etc…

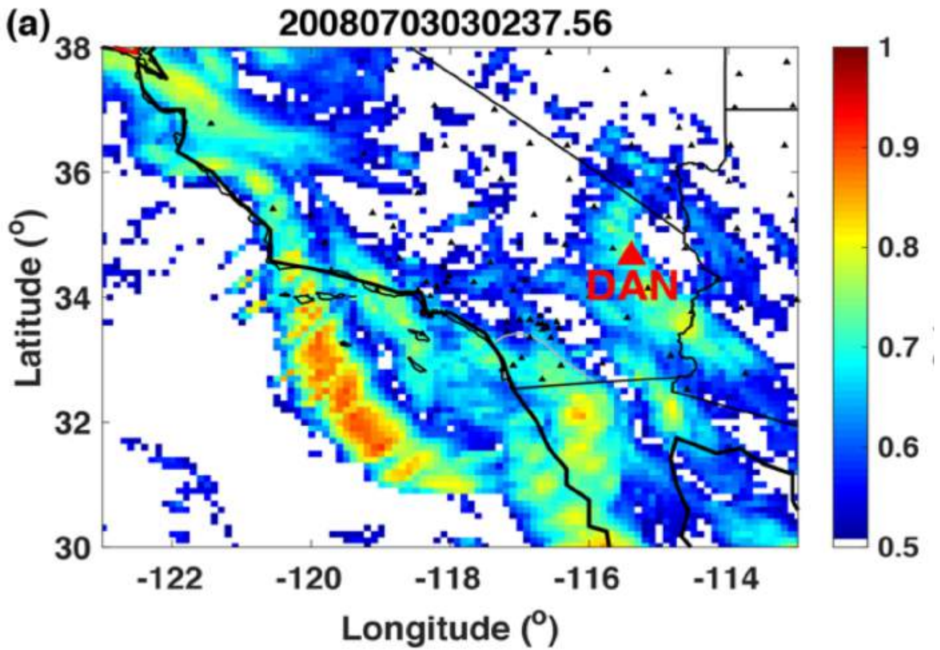

Sharp discontinuities and basin edges

Williams et al. (Poster #023)

New imaging techniques can improve shallow crust velocity models, and in turn the accuracy of High-F simulations

Including inter-frequency correlation into the SDSU BBP Module

Before

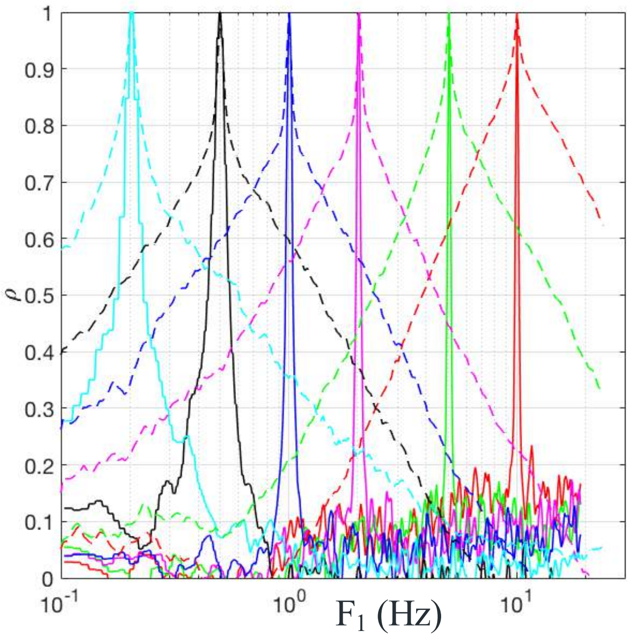

Wang et al. (Poster #010)

Loma Prieta (50 realizations)

—— Simulated

- - - - Empirical

The inter-frequency correlation of epsilon is important for structural risk applications.

Data reveal that neighboring frequencies are generally correlated.

The inter-frequency correlations are well simulated by our post-processing method.

After

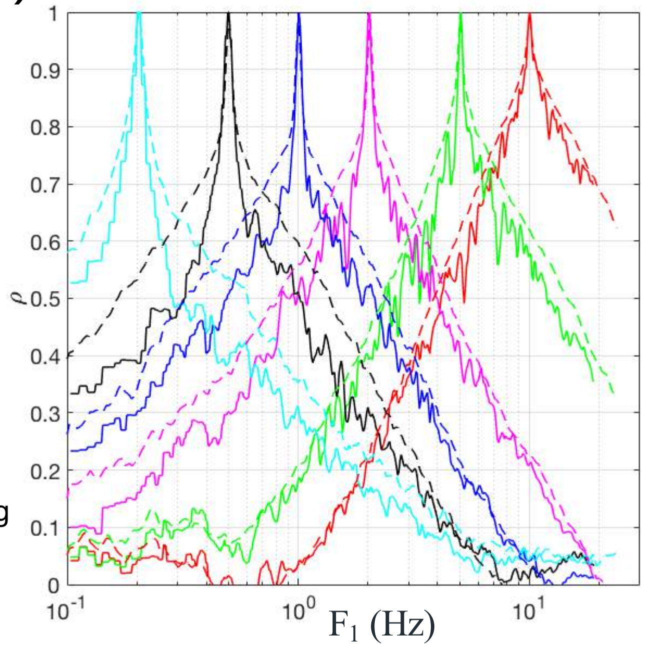

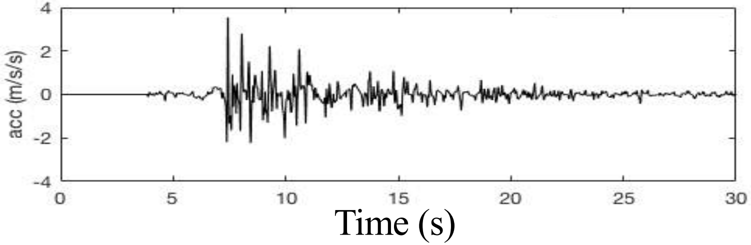

Accelerations at station 8001–CLS

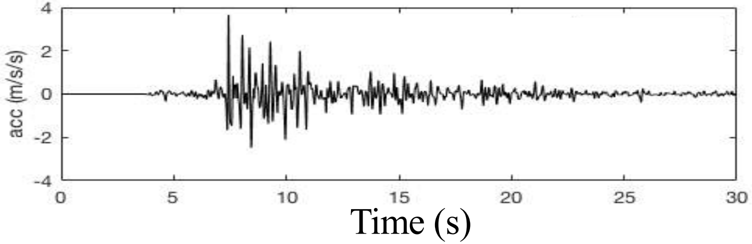

Theme C. Characterizing Seismic Hazards

9. Probabilistic Seismic Hazard Analysis
10. Operational Earthquake Forecasting
11. Earthquake Early Warning
12. Post-Earthquake Rapid Response

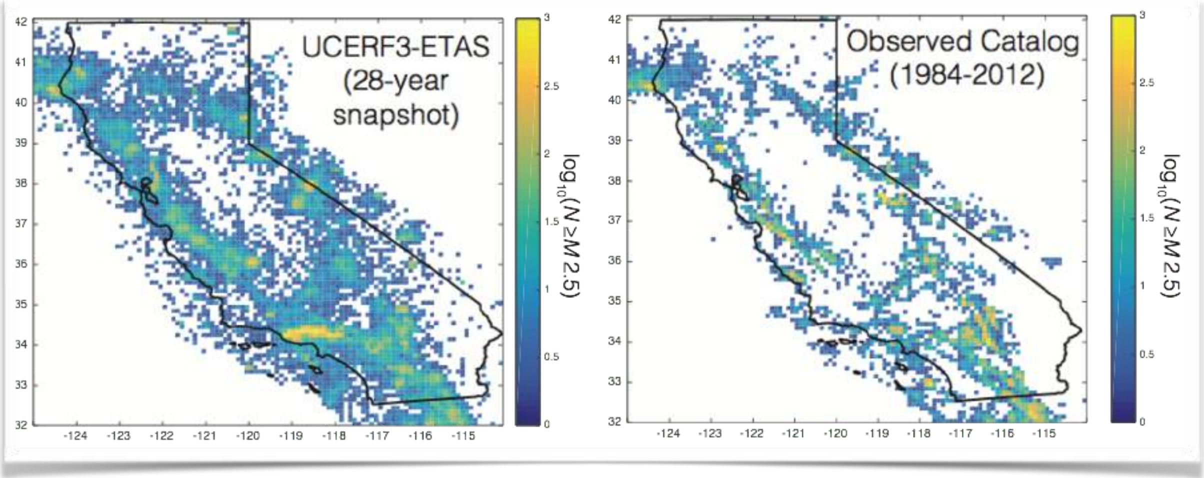

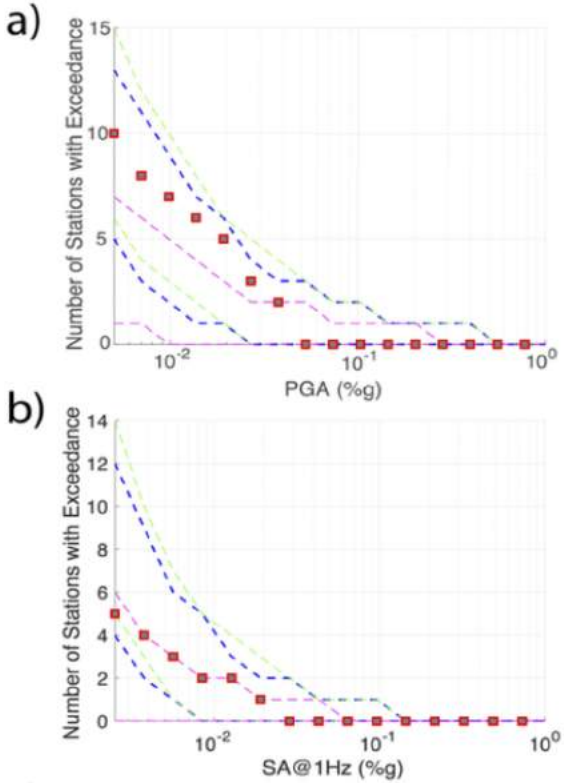

Use of CyberShake ground motions for engineering analysis

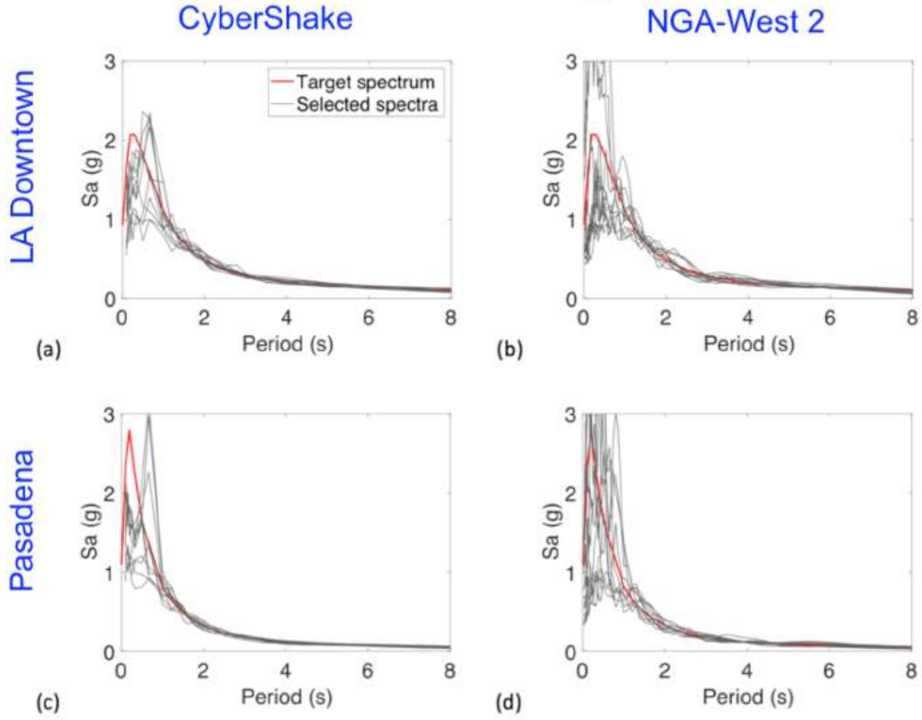

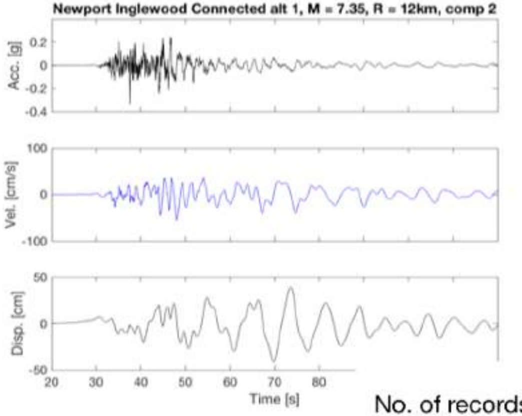

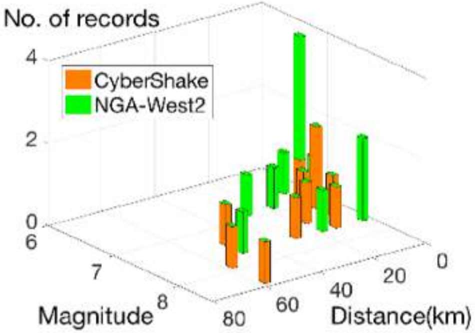

The CyberShake motions appear suitable for engineering evaluation of tall buildings, per the ASCE/SEI 7-16 design standard

Teng & Baker (Poster #006)

CyberShake 15.4 and 17.3 Validation

$$\ln y_{cs} = b_1 + b_2\cdot(m-6) + b_3\cdot(m-6)^2 + (b_4 + b_5\cdot(m-4.5))\cdot\ln(\sqrt{R^2+h^2}) + b_6\cdot R + b_7\cdot\ln(\frac{V_{S30}}{760})$$

GMPE is modified from *Boore and Atkinson*, 2008. Hereafter referred as BA.

T=3s	N	b_1	b_2	b_3	b_4	b_5	b_7	h
CyberShake (CS) 15.4	~10^8	4.02	2.13	-0.55	-0.82	0.12	-0.60	4.47
NGA_W2 in southern California	2691	4.87	1.28	-0.27	-1.36	0.20	-1.18	4.86

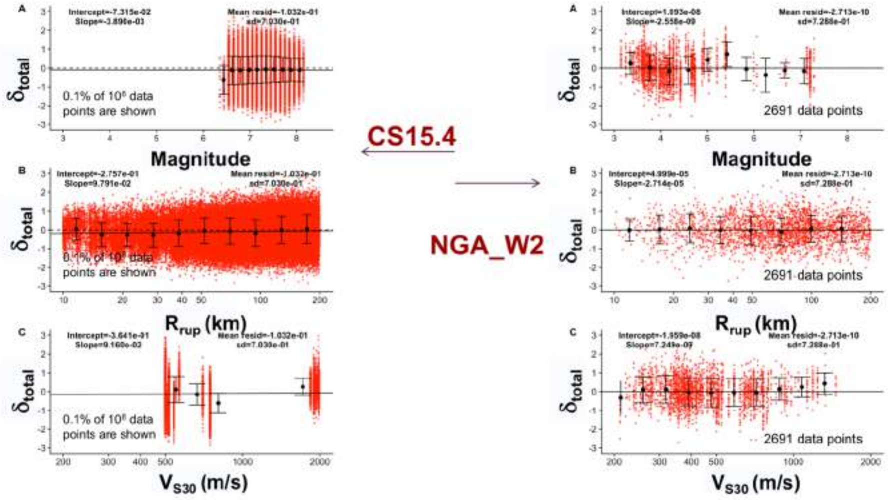

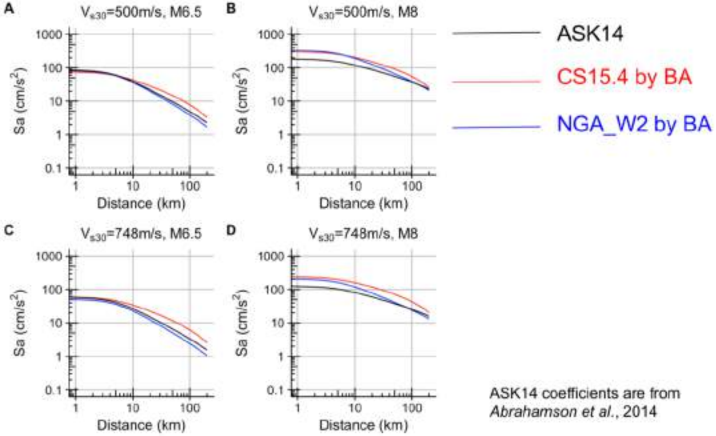

ASK14 coefficients are from *Abrahamson et al.*, 2014

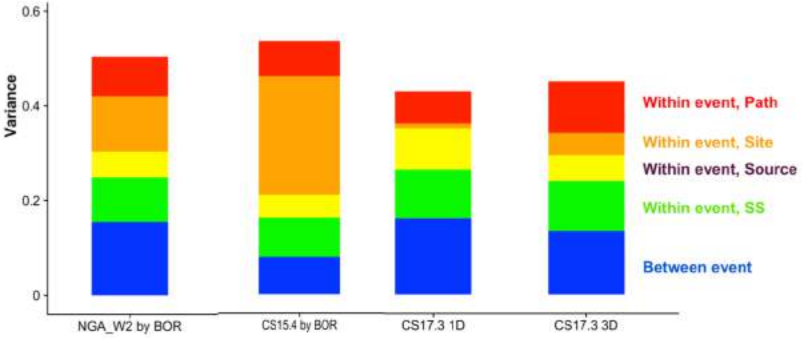

Meng et al. (Poster #024)

CyberShake Study 18.8 Northern CA

Science Collaboration with USGS
Several science and technical participants

180 x 390 km
869 sites (32 overlap with 17.3)

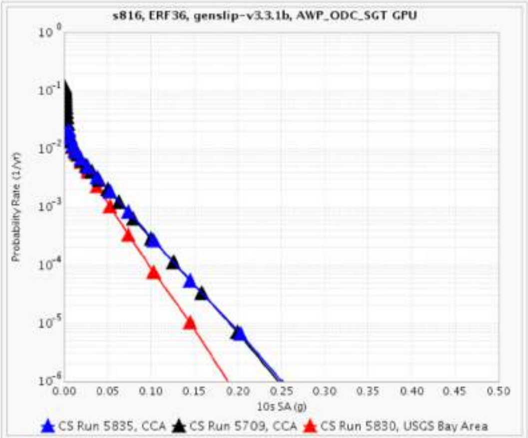

Black=Study 17.3, Red=USGS/CCA/CVM-S4.26, Blue=CCA/USGS/CVM-S4.26

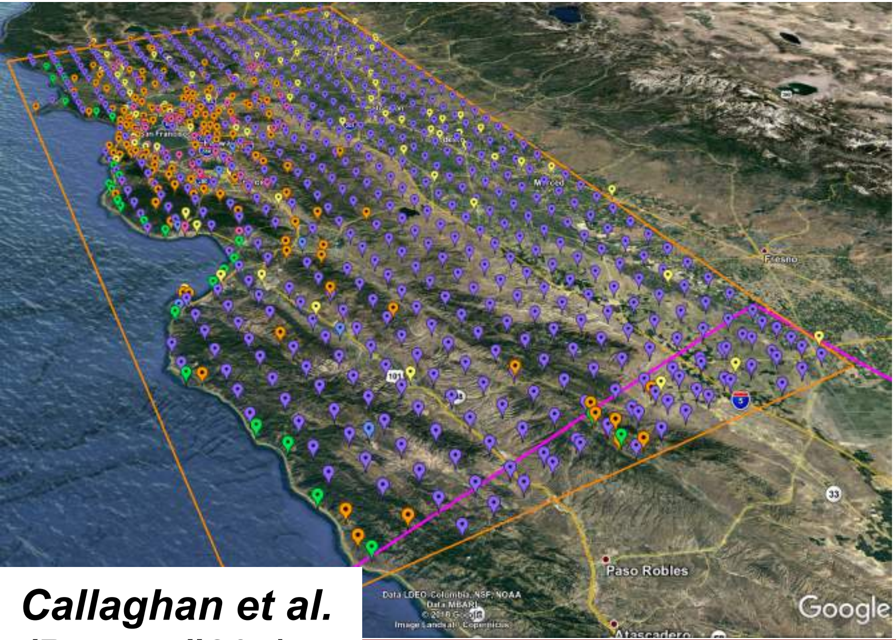

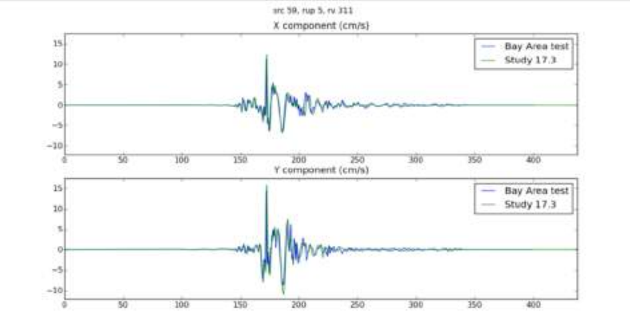

Callaghan et al. (Poster #295)

Started on Friday, August 17, 2018 at 20:17:46 PDT. We are hoping to complete the study by October 1.

Collaboratory for Interseismic Simulation and Modeling (CISM)

Kevin Milner, Bruce Shaw, Jacqui Gilchrist, Tom Jordan, Keith Richards-Dinger, Jim Dieterich, Yifeng Cui, Dmitry Pekurovsky

Fully physics-based PSHA with rupture slip-time histories from RSQSim and 3-D deterministic ground motion simulations from CyberShake

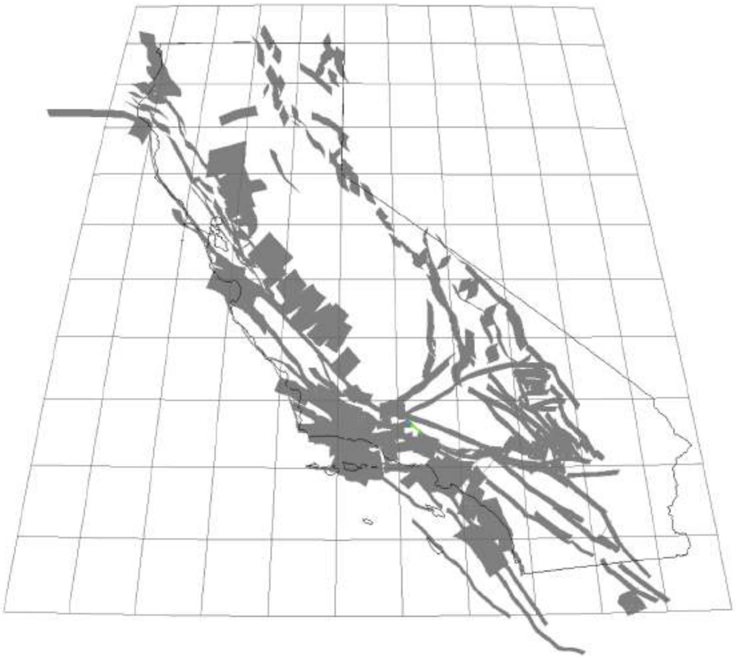

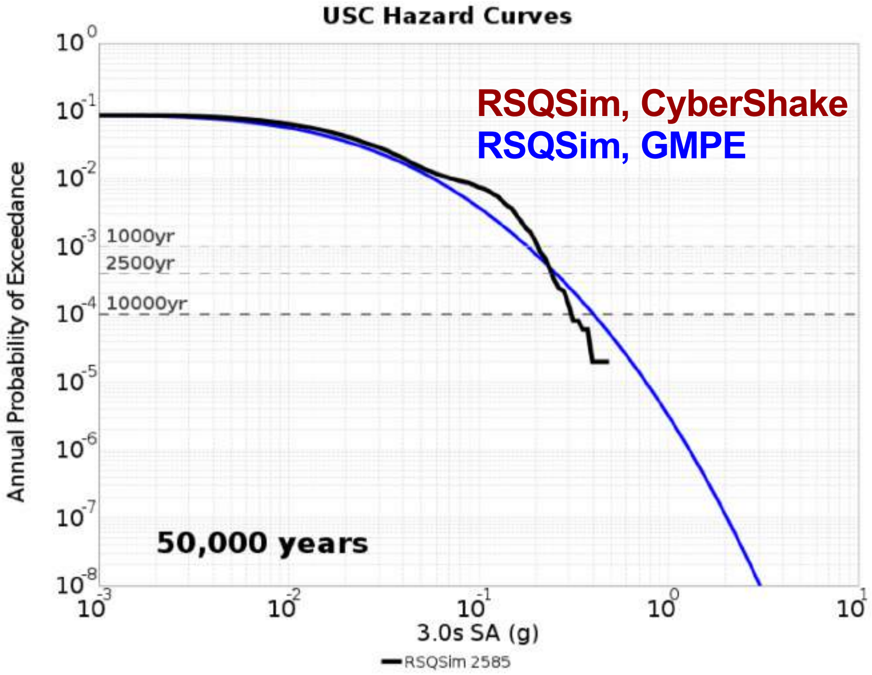

(Posters #031-032)

Working Group on California Earthquake Probabilities (WGCEP)

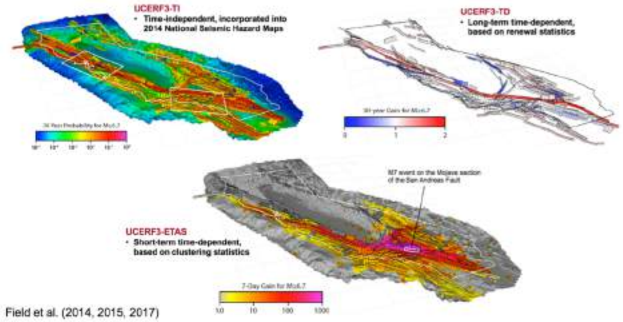

UCERF3-ETAS

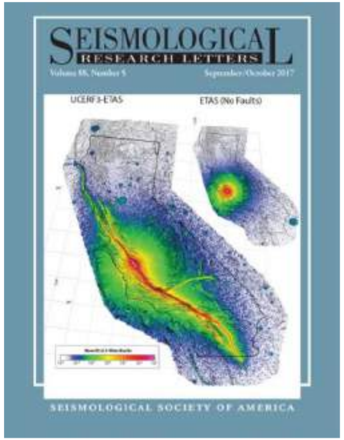

- **UCERF3-ETAS paper published: "Candidate Products for Operational Earthquake Forecasting Illustrated Using the HayWired Planning Scenario…." (Field & Milner, 2018, SRL).**
- **UCERF3-ETAS was formally evaluated by NEPEC in Oct 2017 and they recommended operationalization on an on-demand basis (not automated)**
- **UCERF4 planning paper in press in *SRL*: "Improving Earthquake Rupture Forecasts (Using California as a Guide)"**
- **Fourth Powell Center meeting was held in February to address model testing, which led to a number of proposed milestones for CSEP2**
- **Based on work in the CISM project, paper has been published comparing RSQSim-implied hazard calculations to that for UCERF3 (Shaw et al.,2018, Sci. Advances).**

Collaboratory for the Study of Earthquake Predictability (CSEP)

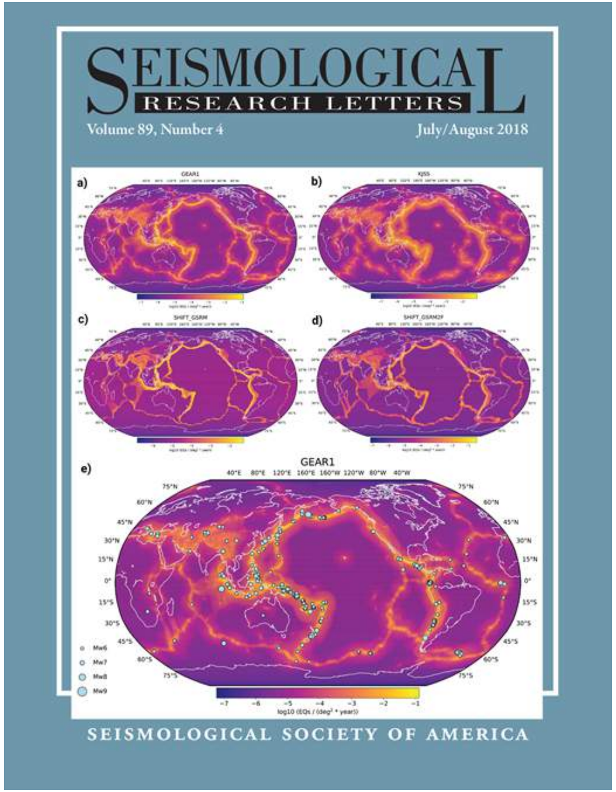

Savran et al. (Poster #033)

SRL Focus Section July/August 2018
guest-editors Andy Michael & Max Werner

1. *Schorlemmer et al*: **The Collaboratory for the Study of Earthquake Predictability: achievements and priorities.**
2. *Cattania et al*: **The forecasting skill of physics-based seismicity models during the 2010-2012 Canterbury, earthquake sequence.**
3. *Bird*: **Ranking global forecasts with the Kagan information score**
4. *Jackson*: **Testing the classic 1988 forecast**
5. *Rhoades et al*: **Highlights from the first ten years of the New Zealand earthquake forecast testing center.**
6. *Taroni et al*: **Prospective CSEP evaluation of 1-day, 3-month, and 5-year earthquake forecasts for Italy.**
7. *Strader et al*: **Prospective evaluation of global earthquake forecast models**
8. *Akinci et al*: **Ensemble smoothed seismicity models for the new Italian probabilistic seismic hazard map.**
9. *Ogata et al*: **Exploring magnitude forecasting of the next earthquake**

Theme D. Reducing Seismic Risk

13. Risk to Distributed Infrastructure
14. Earthquake Physics of the Geotechnical Layer

Shallow stochastic heterogeneity

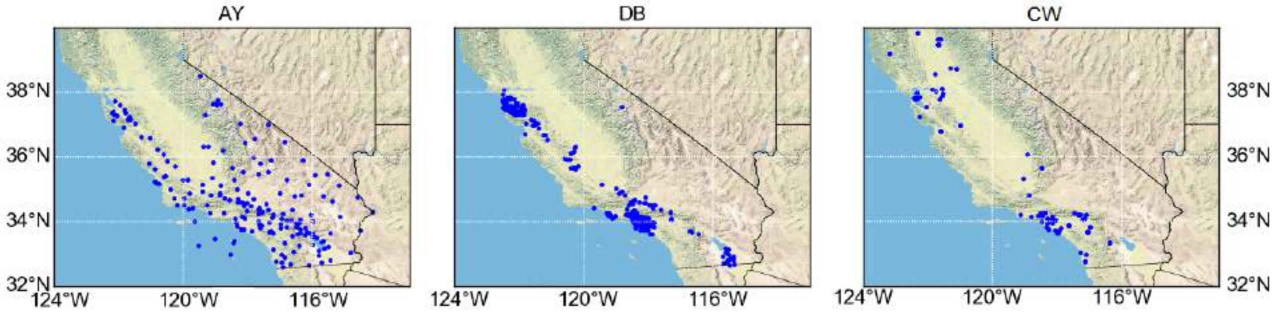

Asimaki, Shi, and Taborda #271

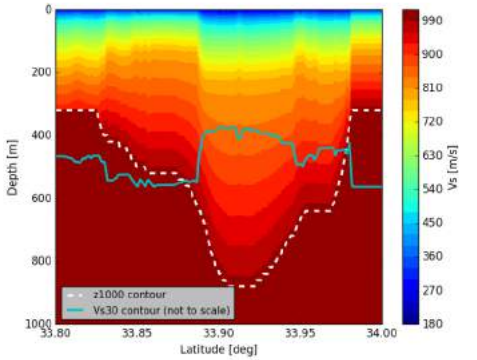

Spatial correlations in ground motion simulations

Puente Hills M 7.05 CyberShake

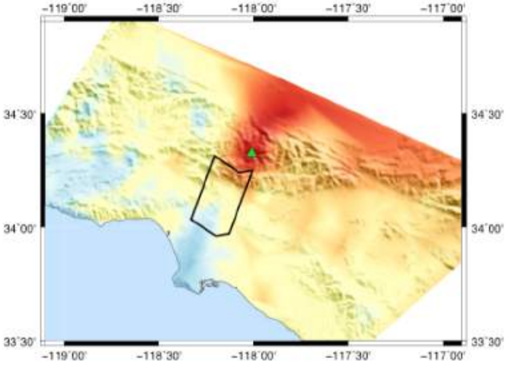

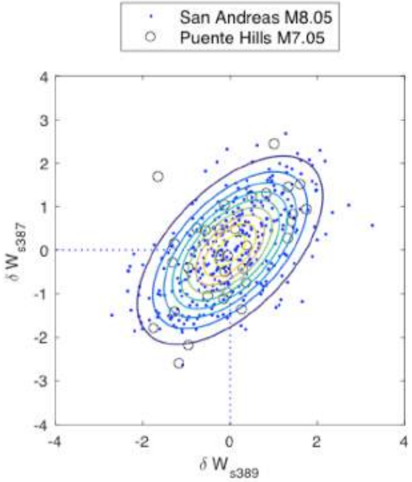

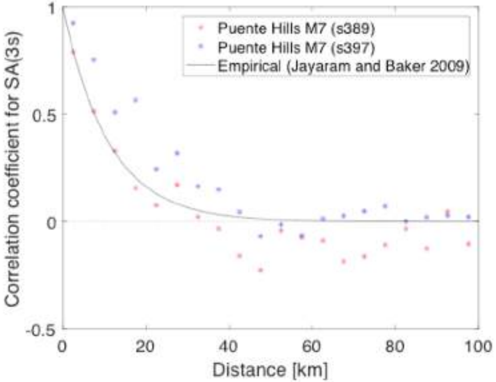

San Andreas M 8.05 CyberShake

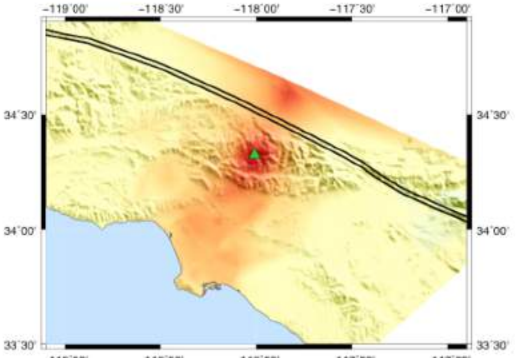

Empirical model

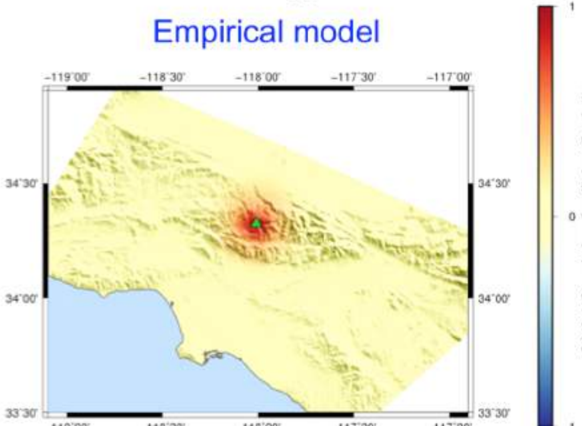

CyberShake simulations enable controlled study of the role of rupture and path effects on spatial correlations—an important property for infrastructure risk evaluations.

Chen & Baker (Poster #007)

Enhanced BBP capabilities

Among others: Fourier-based spectral amplification ratios

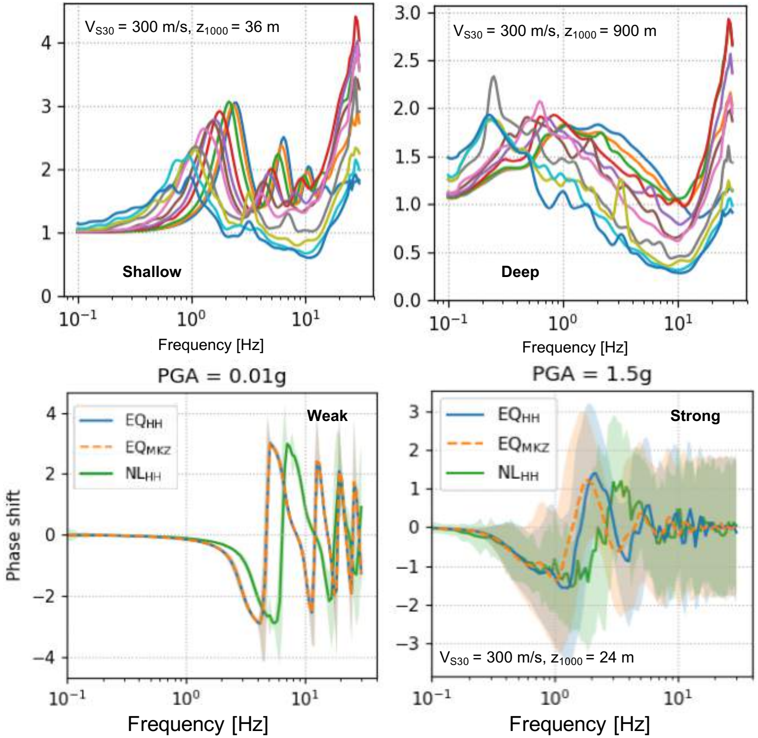

Nonlinear synthetic complex amplification ratios

Asimaki & Shi (Poster #012)

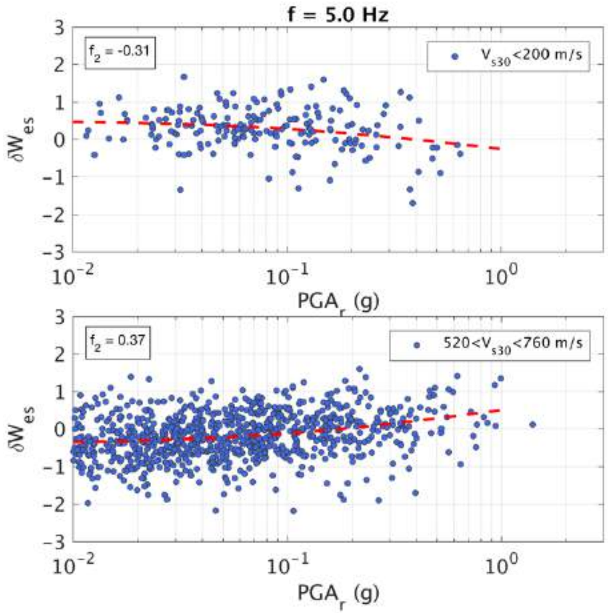

Empirical FAS using NGA-West 2 motions

Bayless & Abrahamson (Poster #011)

Fourier amplification ratios to modify BBP time-series on rock-outcrop; complement efforts to stir GMPE site factors towards Fourier

SCEC-UGMS tool is now publicly available online

https://data2.scec.org/ugms-mcerGM-tool_v18.4/

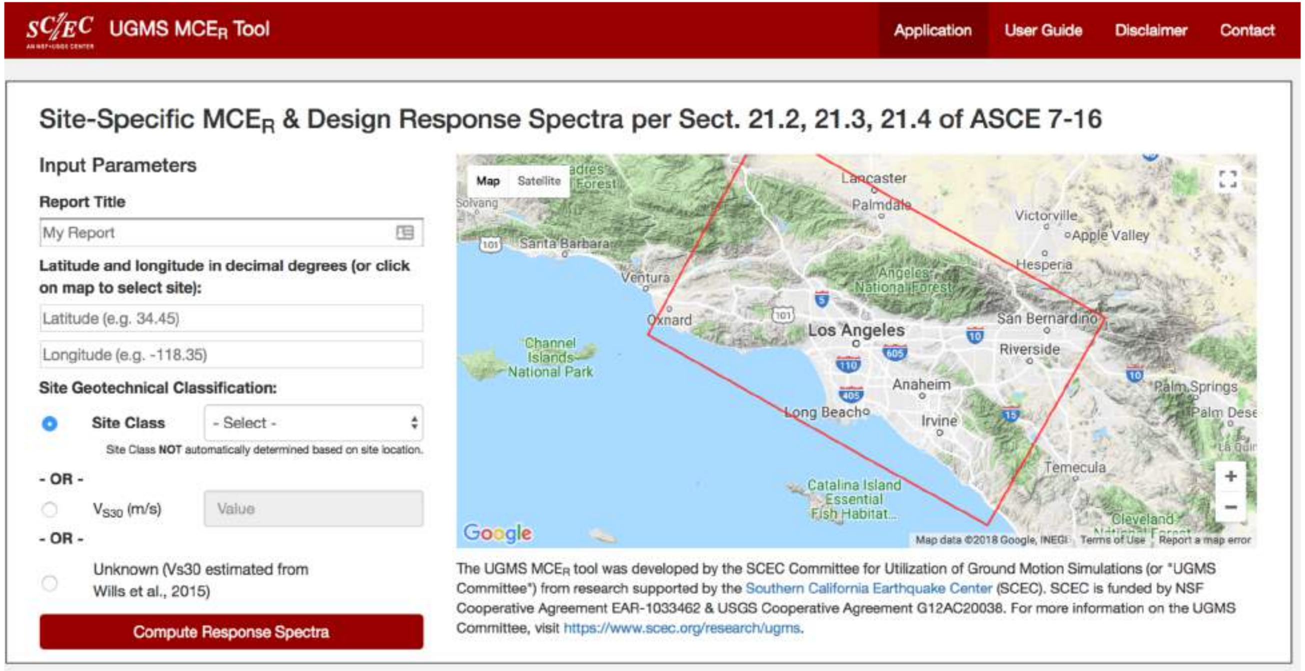

Pauk et al. (Poster #297)

Inclusion of CyberShake results into building code approach to design ground motions for tall buildings.

LA2018

11th National Conference on Earthquake Engineering

integrating science, engineering, & policy

EERI EARTHQUAKE ENGINEERING RESEARCH INSTITUTE JUNE 25th - 29th LOS ANGELES

SCEC as co-organizer with EERI

1200+ registrants

800+ papers

Very strong SCEC presence

- Organization
- Publicity and media relations
- Technical presentations

SCEC Ground Motion Simulations and Engineering Applications Workshop

MONDAY, JUNE 25, 2018

09:00 - 09:10	Welcome and Introduction (PDF, 2.2MB)	Christine Goulet
09:10 - 09:40	Overview of Ground Motion Simulations: Physics and Modeling Alternatives (PDF, 6.7MB)	Robert Graves
09:40 - 10:00	SCEC Simulation Platforms, Validation Objectives and Techniques (PDF, 1.6MB)	Christine Goulet
10:00 - 10:20	CyberShake Validation - Part 1 (PDF, 1.2MB)	Kevin Milner
10:20 - 10:45	CyberShake Validation - Part 2 (PDF, 3.9MB)	Xiaofeng Meng
10:45 - 11:00	*Break*	
11:00 - 11:30	Using CyberShake to Define MCE_R for Tall Buildings (PDF, 3.6MB / PPSX, 49MB)	C.B. Crouse
11:30 - 11:50	Selected Set of CyberShake Seismograms (PDF, 2.6MB)	Jack Baker
11:50 - 12:15	Verification and Validation of Ground Motion Simulations from a 3D Modeling Perspective (PDF, 3.1MB)	Ricardo Taborda
12:15 - 13:00	*Lunch*	
13:00 - 13:30	Broadband Platform (BBP) Validation for Pseudo-Spectral Acceleration (PDF, 8.5MB)	Kathryn Wooddell
13:30 - 13:45	Introduction to Ground Motion Simulation Validation Technical Activity Group (GMSV TAG) (PDF, 2.8MB)	Sanaz Rezaeian
13:45 - 14:30	Utilization of Simulated Ground Motions for Nonlinear Dynamic Analyses of Tall Buildings (PDF, 8.2MB)	Gregory Deierlein
14:30 - 14:45	*Break*	
14:45 - 15:00	Access to Selected Subset of Simulated Ground Motions (PDF, 145KB)	Ting Lin
15:00 - 15:15	Access to Simulated Ground Motions from the GMSV Project Through the NHERI-CI portal (PDF, 6.4MB)	Silvia Mazzoni
15:15 - 15:50	New and Alternative Ideas on Validation Metrics (PDF, 3,7MB)	Farzin Zareian
15:50 - 17:00	Discussion and Period of Questions with Panel	All

W.M. KECK FOUNDATION

USGS science for a changing world

National Science Foundation

U.S. DEPARTMENT OF ENERGY

PG&E Pacific Gas and Electric Company

NCSA

BLUE WATERS SUSTAINED PETASCALE COMPUTING

XSEDE Extreme Science and Engineering Discovery Environment

USC ITS Information Technology Services

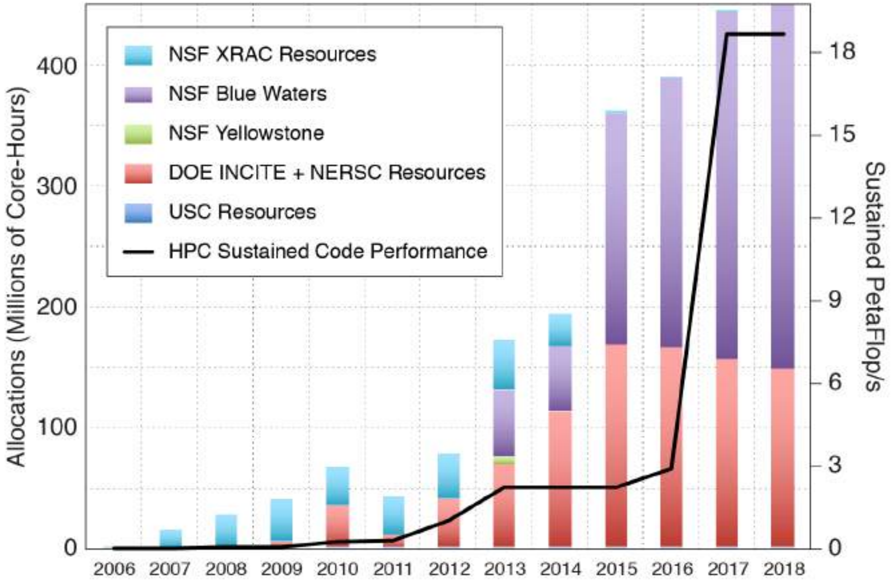

Argonne ALCF

OLCF Oak Ridge Leadership Computing Facility

NCCS.GOV National Center for Computational Sciences

U.S. DEPARTMENT OF ENERGY INCITE LEADERSHIP COMPUTING

NICS

PITTSBURGH SUPERCOMPUTING CENTER

intel

pegasus

Open Science Grid

TACC

NWSC NCAR-Wyoming Supercomputing Center

SDSC

IBM

NVIDIA

CRAY